THE ROLE OF THE MAIZE GENES *MINI-ME* AND *GRASS* IN ESTABLISHING PLANT ARCHITECTURE

By

SHARON TAN CHENG SZE

A THESIS PRESENTED TO THE GRADUATE SCHOOL
OF THE UNIVERSITY OF FLORIDA IN PARTIAL FULFILLMENT
OF THE REQUIREMENTS FOR THE DEGREE OF
MASTER OF SCIENCE

UNIVERSITY OF FLORIDA

2012

In memory of my grandmother

ACKNOWLEDGMENTS

I would like to thank my advisor Dr. Wilfred Vermerris for his patience, wisdom, and knowledge to guide me in my learning experience. To my committee members: Dr. Karen Koch, Dr.Don McCarty, Dr. Pamela Soltis, and Dr. Stuart McDaniel for their guidance and advice. I would like to thank past and current members of the Vermerris lab, Dr. Ana Saballos, Timothy Foster, Annie Greene, and Randi Wheeler, Dr. Chip Hunter from the Koch lab for the help in generating and analyzing the *Mu*-library for the mutants, Frederico Martin from the Settles lab for their help in generating the SNP results from the *grass* F2 population, Forestry lab for allowing me to use their microscope, and Dr. Maria Gallo for allowing me to access her lab to use plant incubator and microscope. I also would like to express my gratitude to my family and friends for their emotional and financial support. I am grateful to the Plant Molecular and Cellular Biology Graduate Program for financial support.

TABLE OF CONTENTS

page

LIST OF TABLES

LIST OF FIGURES

LIST OF ABBREVIATIONS

DAP	Days After Planting
DNA	Deoxyribonucleic Acid
dsDNA	Double-stranded DNA
FAA	Formalin-Acetic Acid-Alcohol
FAD	Flavin Adenine Dinucleotide
NADPH	Nicotinamide Adenine Dinucleotide Phosphate
PCR	Polymerase Chain Reaction
SNP	Single Nucleotide Polymorphism
SSR	Simple Sequence Repeat
TAIL	Thermal Asymmetric Interlaced

Abstract of Thesis Presented to the Graduate School
of the University of Florida in Partial Fulfillment of the
Requirements for the Master of Science

THE ROLE OF THE MAIZE GENES *MINI-ME* AND *GRASS* IN ESTABLISHING PLANT ARCHITECTURE

By

Sharon Tan Cheng Sze

August 2012

Chair: Wilfred Vermerris
Major: Plant Molecular and Cellular Biology

The maize Uniform*Mu* population is a large population of mutants induced by the highly mutagenic *Mutator* (*Mu*) transposable element system. The uniformity in the genetic background was achieved by recurrent backcrossing of a *Mutator* line to inbred line W22. *Mutator* elements transpose to unlinked sites in the genome. The mutants *mini-me* and *grass* were identified from a screen of the Uniform*Mu* population. Both mutants are extreme dwarfs, lack a main stem, and form multiple tillers. The *mini-me* mutant is slightly larger than the *grass* mutant. Under some conditions, the *mini-me* mutant will form hermaphrodite floral structures that are, however, not fertile. Both mutant phenotypes are inherited in a manner consistent with a single recessive mutation.

The purpose of this research was to 1) investigate the causal mutation(s) in the maize *mini-me* and *grass* mutants and 2) use microscopic analysis to analyze in detail the morphological and anatomical features of the mutants.

Since *Mutator* insertions were the most likely cause of the *mini-me* and *grass* mutations, the methods *Mu*TAIL and *Mu*-454 were used to generate libraries of *Mu* flanking regions from *mini-me* and *grass*. A total of 65 sequences were tested for co-

segregation with the mutant phenotypes, but none of the unique sequences tested co-segregated. Given the phenotypic similarities, crosses to test for allelism between *grass* and *mini-me* were performed.

The tiller formation in the mutants appears to be caused by the formation of multiple meristems post-embryogenesis. The small size of the mutant plants is caused by a smaller number of cells, rather than by reduced cell size. Detailed analysis of the leaves revealed that the regular patterning observed in the epidermis of the wild-type maize leaves is disrupted in both mutants. In addition, abnormalities in the differentiation of the vascular bundles, bundle sheaths cells and leaf parenchyma cells in the leaves were observed. Based on these complex phenotypes of both mutants, the *Grass* and *Mini-me* genes are hypothesized to be involved in meristem development and/or cell differentiation.

CHAPTER 1
GENETICS AND PHYSIOLOGY OF PLANT GROWTH AND DEVELOPMENT

Introduction

Population growth, climate change, and the need for alternative fuels from plants as oil supplies are expected to dwindle have put pressure on agricultural production systems. These developments will require rapid adaptations to plant composition, metabolism, and architecture so that plants can continue to provide food, feed, fuel, fiber, and medicines (Sticklen, 2008). Progress in plant biology has increased significantly due to advances in technology, including the ability to sequence whole-plant genomes, with *Arabidopsis* (*Arabidopsis* Genome Initiative, 2000), rice (Goff *et al.*, 2002; Yu *et al.*, 2002), poplar (Tuskan *et al.*, 2006), maize (Schnable *et al.*, 2009), and sorghum (Paterson *et al.*, 2009) representing several key plant genomes. Additional resources include *Brachypodium distachyon* (The International Brachypodium initiative, 2010), grapevine (Jaillon *et al.*, 2007), cucumber (Huang *et al.*, 2009) and strawberry (Shulaev *et al.*, 2011), as part of a growing list. With these new resources, scientists are able to more efficiently relate gene sequence to gene function, and to identify gene networks involved in complex metabolic and developmental processes.

With the increased knowledge of plant development and its genetic control, we have the ability to modify plants so that food and biomass production can be optimized. For example, biomass production may be enhanced by reducing grain production or grain production may be enhanced by reducing biomass production. Modification of plant architecture can also increase the ability to capture photosynthetically active radiation (PAR) (Fourcaud *et al.*, 2008). The grain yield of maize (*Zea mays* L.) has continued to increase over time, in part due to its tolerance to high planting density. This

required adaptation of plant architecture, specifically the leaf angle, which is evidenced by the more erect leaves of modern maize hybrids (Zhu *et al.*, 2010).

Growing food crops for biofuels is not sustainable in the long run, due to the need to produce more food for a growing population, while widespread hunger in developing countries creates ethical concerns about the use of food crops for the production of fuels (Tenenbaum, 2008). A possible way to meet the increased demand for bio-fuels is the use of vegetative residues such as corn stover for the production of cellulosic biofuels. In addition, cellulosic biofuels can be produced from biomass crops grown on land that is not suitable. for the production of food crops. Cellulosic fuels are produced from the unused portion of a plant, such as corn stover, sugarcane bagasse, or from dedicated biomass crops such as miscanthus and switchgrass. The biomass is collected and delivered to a biofuel plant, pretreated with heat and chemicals to make cellulose accessible to enzymes, hydrolytic enzymes then break down the sugars, and microbes ferment the sugars into ethanol. The ethanol is distilled and distributed for use (Sticklen, 2008).

Crop plants such as rice, wheat, and maize have been bred mostly for enhanced grain yield, while biomass yield and composition have not been taken into much consideration. For example, rice has good grain yield but is low in biomass yield (Jahn *et al.*, 2011). A better understanding of plant development and its genetic control may lead to crops that can simultaneously meet the increasing demand for food and fuel.

Embryogenesis

Seed formation in flowering plants results from sexual fertilization of the haploid megagametophyte (female) by a haploid microgametophyte (male) produced in the flowers of mature plants. Fertilization results in the formation of an embryo and

endosperm with the full complement of chromosomes. Two main phases can be identified during plant embryo development. First, the basic cellular patterning of the root and shoot body are formed, followed by post-embryonic development involving embryonic cell growth as well as storage of starch, oils, and proteins for the embryo, which are needed during germination and the early seedling stage (Goldberg *et al*., 1994). An initial asymmetric division of the diploid embryo results in a small apical cell and a large basal cell. After this first division, the cells divide along random planes with establishment of the radial axis and bilateral symmetry (West *et al.*, 1993, Wang *et al.*, 2008). Most of the seed is taken up by the endosperm, which is formed from two polar nuclei in the central cell of the embryo sac and one sperm nucleus to generate a triploid (3n) tissue (Ohad *et al.*, 1996) containing starch and storage proteins. The maize embryo is located on the adaxial side of the endosperm. Once the body plan has been established and important storage reserves have been accumulated, the embryo will go into developmental arrest until germination.

Embryo and seed development are very complex processes and involve the coordinate expression of many genes. Consequently, if the function of any of these genes is disrupted, the embryo may not form properly. Studying the phenotype of the mutants in which genes involved in embryo development that do not function properly can reveal the normal function of these genes. Examples of this approach led to the identification of the following Arabidopsis genes involved in embryo patterning: *WUSCHEL (WUS)*, *CUP-SHAPED COTYLEDON* (*CUC*), *SHOOTMERISTEMLESS* (*STM*), and *DORNRÖSCHEN* (*DRN*). The WUS transcription factor regulates stem cell identity (Mayer *et al.*, 1998). The CUC gene activates *STM* to complete the separation

of the apical-basal plane (Galinha *et al.*, 2009). The *CUC* gene is required for cotyledon separation and activates *STM* to form shoot apical meristem (Aida *et al.*, 1997) with *DRN* also redundantly controlling cotyledon formation (Kirch *et al.*, 2003).

Phytohormones

Phytohormones are small molecules present in low concentrations that mediate growth and development. Several distinct classes of compounds have been identified such as auxin, cytokinin, gibberellic acid, abscisic acid, ethylene, strigolactones, and brassinosteroids.

The role of the phytohormones auxin, brassinosteroids, cytokinin, ethylene, and gibberellic acid (GA) in regulating plant growth and development have been studied extensively (reviewed Teale *et al.* 2006). Below follows a brief summary of how mutants affected in their ability to synthesize, transport or recognize the different classes of plant hormones have been used to elucidate the mechanisms of hormone action.

Auxin

Auxin is mostly present in the form of indole-3-acetic acid (IAA) (Zhao, 2010) and can be synthesized via a tryptophan-dependent pathway and a tryptophan-independent pathway. Auxin induces cell elongation in stems.

Auxin suppresses outgrowth of axillary buds (Leyser, 2003) as evidenced by the phenotype of the Arabidopsis *auxin resistant1* (*axr1*) mutant, which has many branches compared to the wild type (Lincoln *et al.*, 1990). Reduced auxin transport increases tillering in rice as shown in *PINFORMED1* (Os*PIN1)* mutants (Xu *et al.*, 2005). The understanding of the pathway of *de novo* auxin biosynthesis is incomplete. A family of 11 *YUCCA* (*YUC*) flavin monooxygenases was identified in Arabidopsis. The genes were shown to be expressed mainly in the meristems, young primordia, vascular tissues

and reproductive organs (Cheng *et al.*, 2006), suggesting those are the sites of auxin synthesis. The role of *YUCCA* genes in tryptophan-dependent auxin biosynthesis was demonstrated through the analysis of the dominant Arabidopsis *yucca1-D* mutant, identified through T-DNA activation tagging. The mutant plant had elongated hypocotyls due to overproduction of auxin and was able to produce many roots on auxin-free medium, unlike the wild-type control. The mutant phenotype was restored by overexpression of the bacterial *iaaL* gene, which resulted in the formation of conjugates between free IAA and lysine, thereby reducing the levels of free auxin, and masking the *yucca* phenotype. The YUCCA1 protein contains conserved motifs for binding flavin-adenine dinucleotide (FAD) and NADPH, and is involved in the N-oxygenation of tryptamine, formed from tryptophan (Woodward *et al*., 2005, Cheng *et al*., 2006).

In maize, *Sparse inflorescence 1* (*Spi 1*) is essential for localized auxin biosynthesis. *Spi1* encodes a monocot-specific *YUC* gene family member. The *spi 1* mutant exhibits defects in the formation of branches, spikelets, florets, and floral organs (Gallovotti *et al.*, 2008). Cheng *et al.* (2006) demonstrated gene redundancy in the Arabidopsis *YUC* genes by generating triple and quadruple mutants in Arabidopsis and showing that knockouts of four genes were required to generate a mutant phenotype similar to *spi 1* in maize.

The degradation of auxin is better understood than its biosynthesis. The AUXIN RESISTANT1 (AXR1) protein is essential for proper conjugation of the SCF. F-box proteins with Skp1 and Cdc53 (cullin) form ubiquitin ligase complexes called SCFs. The Transport Inhibitor Response 1 (TIR1) encodes an F-box, an auxin receptor that interacts with SCF (Dharmasiri *et al.*, 2005). Proteasome-mediated auxin degradation

involves SCF^{TIR1} that degrades AUX/IAA proteins that are repressors to AUXIN RESPONSE FACTOR (ARF) in a high auxin environment. Mutations in AXR1 exhibit increased branching with fewer lateral roots, and reduced fertility. As a consequence, mutant AXR1 protein cause defects in downstream auxin responses due to improper conjugation of SCF to enable proper degradation of AUX/IAA proteins (Lincoln *et al.*, 1990, Leyser *et al.*, 1993, Gray *et al.*, 2001, del Pozo *et al.*, 2002).

Gibberellin (GA)

Gibberellin was initially isolated from *Giberella fujikuroi,* a pathogenic fungus (reviewed by Phinney 1983) promotes cell elongation. There are more than 125 characterized compounds in the GA family but only a few GAs - GA_1, GA_3, GA_4, GA_5, GA_6, and GA_7 – have been shown to be biologically active (reviewed by Sponsel and Hedden, 2010).

Figure 1-1 shows examples of *gibberellic acid* (*ga*) mutants that are affected in various steps of the GA biosynthesis pathway. Some of these mutants are severely reduced in height and display variation in tillering.

The rice *gibberellin-insensitive dwarf 1* (*gid1*) lacks a soluble gibberellin receptor. The molecular mechanism of this receptor is unclear (Ueguchi-Tanaka et al., 2005). The mutant has a severe dwarf phenotype and is unresponsive to GA. The *GID1* gene was cloned with positional cloning. Using the yeast two-hybrid system, the GID1 protein was shown to interact with SLENDER1 (SLR1) only in the presence of GA (Ueguchi-Tanaka at al., 2005).

Cytokinin (CK)

The natural form of cytokinin in maize plants is zeatin. It is found in meristematic regions and growing plant tissues and promotes cell division and differentiation (Mok and Mok, 2001).

Cytokinin signaling involves a phosphotransfer cascade (Inoue *et al.*, 2001). An example of an Arabidopsis mutant involved in the CK signaling pathway is *cytokinin response1* (*cre1*). This mutant was identified by screening a population of mutants induced with ethyl methanesulphonate (EMS). Introduction of the wild type *CRE1* gene into a *cre1* mutant plant restored normal plant growth (Inoue *et al*., 2001). To test for signaling function, the yeast *Synthetic Lethal of N-end rule* (*SLN1*) gene was replaced with the *CRE1* gene from Arabidopsis. The *SLN1* gene encodes an osmosensing histidine kinase in yeast. Without proper function of *SLN1*, the mitogen-activated protein (MAP) kinase pathway is always activated which is lethal to yeast cells (Inoue *et al.*, 2001). When *CRE1* was introduced into the yeast system, the function was restored showing normal plant growth.

The *SHOOTMERISTEMLESS* (*STM*) gene involved in shoot apical meristem (SAM) maintenance in Arabidopsis encodes a homeodomain protein in the *KNOTTED-1* (*KN1*) family (Kerstetter *et al.*, 1994). It was proposed that cytokinin acts upstream of *STM* because of the increasing meristem size when both *STM* and cytokinin levels were overexpressed individually with *CYTOKININ OXIDASE/DEHYDROGENASE* (*CKX*) (Werner *et al.*, 2003). In Arabidopsis, it has been identified that overexpression of *STM* induces cytokinin biosynthesis genes At*IPT5* (isopentenyl transferase) and At*IPT7* (Yanai *et al.*, 2005).

Cytokinin is also involved in branching: *CYTOKININ OXIDASE* (*CKX*) is identified as an enzyme that degrades cytokinin (Sakakibara, 2006). A defect in this gene in rice caused an increase in panicle branch and spikelet number (Ashikari *et al.*, 2005).

Brassinosteroids

Brassinosteroids (BR) are steroidal hormones first isolated from *Brassica napus* (Grove *et al.*, 1979) involved in seed germination and cell elongation. Brassinolide (BL) is the first characterized brassinosteroid from bee-collected rape pollen (Greeve *et al.*, 2000).

The elucidation of BR synthesis and signal transduction was accomplished with the help of Arabidopsis, pea (Nomura *et al.*, 1999), tomato (Bishop *et al.*, 1999; Koka *et al.*, 2000), and rice (Yamamuro *et al.*, 2000) mutants. These mutants were either BR-deficient or BR-insensitive (BRI) and typically displayed dwarfism with abnormal morphology. The signal transduction pathway has been identified with the help of Arabidopsis mutants. It is now known that BRI1 is a receptor-like kinase that interacts with Leucine Rich Repeat-RLK BRI1-ASSOCIATED RECEPTOR KINASE1 (BAK1) and downstream BRI1 KINASE INHIBITOR 1 (BKI1) (Wang *et al.*, 2006).

The Arabidopsis *dwarf1-1* mutant was identified from a mutagenized population and was shown to be a brassinosteroid biosynthetic mutant. The normal phenotype can be restored with exogenous application of brassinosteroids (Choe *et al.*, 1999). The *dwarf1-1* mutant was shown to have a single mutation leading to a reduced ability to bind FAD. The *DWARF1* gene encodes an oxidoreductase that requires FAD as a cofactor to function normally(Choe *et al.*, 1999).

Strigolactones

Strigolactones represent a group of hormones discovered fairly recently. Strigolactones are released from root exudates in plants that promote germination of *Striga,* parasitic plants that infect monocots (Bouwmeester *et al.*, 2007). Unexpectedly, strigolactones are also associated with variation in branching that had been observed in the Arabidopsis *more axillary meristem* (*max*), the pea *ramosum* (*rms*), and the *Petunia hybrida decreased apical dominance* (*dad*) mutants (Arite *et al.*, 2007; Beveridge *et al.*, 1997). *RMS1*, *RMS5*, and *MAX4* encode carotenoid cleavage dioxygenases (Gomez-Roldan *et al.*, 2008). There are also orthologs in rice such as *HIGH TILLERING DWARF1* (*HTD1*), ortholog of *MAX3* (Zou *et al.*, 2006), and *DWARF10* (*D10*), ortholog of *MAX4* (Arite *et al.*, 2007). The mutants that were isolated from rice exhibit high tillering phenotypes with low endogenous levels of strigolactone (Umehara *et al.*, 2008). In order to demonstrate that strigolactone suppresses branching, a synthetic analog of strigolactone, GR24, was applied to rice *dwarf* mutants and *Arabidopsis max* mutants. Upon application, these mutants were restored to the normal phenotype (Umehara *et al.*, 2008). Also, similar mutants in maize deficient in *Carotenoid cleavage dioxygenase8* (*Ccd8*) also demonstrated tillering (Guan *et al*., unpublished data)

The previous sections represent a subset of the mutations affecting levels of hormones involved in plant growth and development. In addition, other hormones and growth regulators such as abscisic acid, ethylene, jasmonic acid, and salicylic acid are important contributors to plant growth and development. The hormones do not work independently of each other, but there is cross talk among hormones that coordinates normal plant growth and development (Weiss, 2007). Although pathways for major hormone biosynthesis, signaling, and perception have been identified, how these

hormones communicate spatially and temporally to regulate plant growth and development remains to be fully elucidated (Durbak et al., 2012).

Genetic Control of Plant Height

Plant height is an important agronomic trait especially in crops plants such as rice, wheat, maize and sorghum, as evidenced by the successes of the 'Green Revolution' in the 1960's reviewed by Khush *et al.* (2001). World-wide food production was able to keep up with the demand of a growing population due to the introduction of dwarfing alleles into rice and wheat. Dwarfing alleles were favorable as they caused a phenotype able to withstand lodging. Severe lodging typically results in the inability to combine harvest the crop, while moderate lodging can alter plant growth and development, including flowering time, result in increased damage from rain or hail, reduce the photosynthetic capability of the plant, and reduce the efficiency of nutrient transport (Khush *et al.*, 2001). One of the dwarfing alleles of wheat was identified through analysis of the *reduced height* (*rht*) mutant. The *Rht* gene encodes a protein resembling a nuclear transcription factor (Peng *et al.*, 1999). The *rht* mutant does not respond well to gibberellin. The *Rht* gene was shown to mediate the signal transduction pathway of gibberellin (GA) and when mutated caused reduced response to GA. The Arabidopsis and maize *Rht* orthologs are *GIBBERELLIN-INSENSITIVE* (*GAI*) (Sasaki *et al.*, 2002) and *Dwarf8* (Anderson *et al.*, 2008) respectively. The orthologs of wheat, *Arabidopsis*, and maize, belong to the GRAS family of proteins (Ikeda *et al.,* 2001). The acronym GRAS was derived from three cloned genes, *GAI*, *RGA* (*REPRESSOR of GA1*), and *SCR* (*SCARECROW*) (Benfey *et al.*, 1993, Peng *et al.*, 1997, Silverstone *et al.*, 1998). The GRAS family of proteins is involved in regulatory roles for plant growth and signaling specific to plants. The GRAS family of proteins share similarity with their two

conserved regions at the N-terminus that include a DELLA domain of 27-amino acids (Willige *et al.*, 2007). DELLA proteins are repressors of plant gibberellin responses (Peng *et al.*, 1997). Another example of a dwarf mutant in rice known as *semidwarf1* (*sd1*) was identified to be defective in GA biosynthesis (Monna *et al.*, 2002). The phenotype of *sd1* can be restored with endogenous GA. The *sd1* gene encodes GA 20-oxidase (GA20ox), an enzyme involved in GA biosynthesis and a major determinant of GA production (Monna *et al.*, 2002).

Another dwarf mutant in maize, known as *brachytic2* (*br2*), has short lower internodes but the ear, tassel, and leaves are not affected in size. The *br2* phenotype could not be restored by endogenous application of auxin, GA, brassinosteroids, or cytokinins, indicating that *br2* is not simply defective in hormone biosynthesis (Multani *et al.*, 2003). Upon cloning using *Mutator (Mu)* transposon-tagging, the *Br2* gene was identified to be highly similar to Arabidopsis *P GLYCOPROTEIN1* (At*PGP1*) (Multani *et al.*, 2003). At*PGP1* is also closely related to adenosine triphosphate (ATP)-binding cassette transporters (ABC-transporter) of the multidrug resistant (MDR) subfamily in humans (Jones *et al.*, 2004). Multani et al. (2003) concluded that *Br2* is involved in polar auxin transport in maize. This was further substantiated by the observations that in Arabidopsis, a mutation in the At*PGP1* gene affects auxin transport in a similar manner as in *br2* (Multani et al., 2003).

Genetic Control of Branching and Tillering

In angiosperms, the apical-basal axis is established during embryogenesis with the formation of the shoot apical and root apical meristems that provides polarity to the plant. Diversity in plant morphology is also the result of the ability to generate axillary branching. The importance of diverse patterns of branching does not only provide

additional surface for a plant to capture light for photosynthesis, but is also an important agronomic trait. For example, research was conducted to investigate differences in plant architecture of cultivated rice (*Oryza sativa*) to a related wild species of rice, *Oryza rufipogon* (Jin *et al.*, 2008). The wild species of rice is short, and has a wide tiller angle, whereas the cultivated species has a near-erect growth form. The traits possessed by cultivated rice are favorable due to the ability to increase photosynthetic efficiency, and allow dense planting because of the erect growth form. The gene responsible for the upright growth in rice was identified as *PROSTRATE GROWTH1* (*PROG1*) through genetic mapping. *PROG1* encodes a 167-residue polypeptide that acts as a transcription factor. It contains a highly conserved C2H2-type zinc-finger motif at its N-terminal region with the activation domain localized at the C-terminus. Following the comparison of the 2.679-kb *PROG1* sequence between the wild species and the cultivated rice, the cause for altered plant architecture was shown to be a nucleotide substitution in the coding region that prevented complete protein binding in cultivated rice. Expression analysis revealed that *PROG1* was localized at the axillary meristems.

Another example of a mutant displaying altered branching patterns is *teosinte branched1* (*tb1*) (Doebley, 1983), a maize mutant with long lateral branches tipped by tassels, and many tillers at the basal node resembling a teosinte plant (*Zea mays* ssp. *parviglumis*), the progenitor of maize. The function of *Tb1* is to suppress lateral branch growth in maize. Further investigation (Doebley *et al.*, 1997, Cubas *et al.*, 1999) proved that *Tb1* encodes a transcriptional regulator, member of class II of the TCP family. The name TCP stands for *Tb1* in maize, *CYCLOIDEA* (*CYC*) in Antirrhinum, and *PFC* (proliferating cell) proteins in rice. The orthologs of *Tb1* were also identified in rice

(Takeda *et al.*, 2003) and sorghum (Doust, 2007a). In Arabidopsis, a mutation in the ortholog of *Tb1*, *TEOSINTE BRANCHED1-LIKE 1* (*TBL1*), caused a hyperbranching phenotype (Finlayson, 2007), showing that the function of *Tb1* is not unique to the grass family.

The maize *corngrass1* (*cg1*) looks like a bush because of the repeated initiation of tillers in the axil of each leaf. The *cg1* mutant was initially proposed to be an ancestral type of maize because of its characteristic to propagate vegetatively (Galinat, 1954). The severe phenotype of *corngrass1* was shown to be caused by two tandem microRNA156 (miR156) genes that are overexpressed in the meristem and lateral organs (Chuck *et al.*, 2007). An estimated thirteen maize genes are targeted by miR156 (Chuck *et al.*, 2007), including genes *SQUAMOSA Promoter-Binding Protein-Like* (*SPL*) encoding plant-specific transcription factors. The other targeted genes are also involved in plant developmental patterning (Rhoades *et al.*, 2002). Similar mutants from maize such as *teopod1* and *teopod2* (Singleton, 1951) exhibit similar tiller phenotype but not as severe as *cg1*.To date, the underlying cause for the *teopod* phenotype is not clear.

The maize mutant *grassy tillers1* (*gt1*) was originally identified in an EMS population. The mutation results in the formation of many tillers. The *gt1* gene was cloned with positional cloning and was shown to encode a class-I homedomain leucine zipper transcription factor (Whipple *et al.*, 2011). The expression of *gt1* was detected in shoot axillary buds using *in-situ* RNA hybridization. The function of the gene is to suppress lateral branching in maize.

Mutagenesis and Transposable Elements

Genome sequences of several plants, including *Arabidopsis* (Arabidopsis Genome Initiative), rice (Goff *et al.*, 2002, Yu *et al.*, 2002), maize (Schnable *et al.*, 2009) and

sorghum (Paterson *et al.*, 2009), have been sequenced, but the sequence data alone are not informative to link genes to their functions. Progress in plant biology still relies heavily on the study of mutants and their causal genes. Mutants can either occur naturally (for example as a result of errors during DNA replication), or result from chemical mutagenesis with, for example, ethyl methane sulfonate (EMS), or from the insertion of transposable elements ("jumping genes"). Mutants are of value in both forward and reverse genetics approaches. Forward genetics is focused on identifying the causal gene underlying a known mutant of interest. Reverse genetics is used to identify the function of a known gene by specifically mutating this gene and observing the resulting phenotype.

Mechanism of Transposition

Transposable elements are DNA sequences that are able to move themselves from one location in the genome to another. Transposable elements were first identified by Barbara McClintock (McClintock, 1947). There are two classes of transposons. Class I transposons are retrotransposons that rely on an RNA intermediate that is reverse transcribed into a DNA copy, which is then inserted in a different location of the genome. Class II transposons are classified as DNA transposons that do not involve RNA intermediates. The class II transposable elements contain autonomous and non-autonomous elements. Non-autonomous elements can only transpose in the presence of an autonomous element. The autonomous elements encode a transposase, which is a protein that enables excision, copying, and insertion ("cut and paste mechanism"). An example is the maize *Activator/Dissociator* (*Ac/Ds*) system (McClintock, 1947), where *Ac* is the autonomous element and *Ds* is the non-autonomous element. These transposable elements have terminal inverted repeats (TIR). The role of terminal

inverted repeats is to act as a recognition site for the transposase encoded by the autonomous element and necessary for transposition.

The other two major transposable element systems of maize are *Enhancer/Initiatior* (*En/I*) (Peterson, 1953), also known as *Suppressor mutator / defective Suppressor mutator* (*Spm/*d*Spm*) (McClintock, 1954), and Robertson's *Mutator* (*Mu*) (Robertson, 1978). The autonomous element is listed first in these above systems.

The Major Transposable Element Systems in Maize

Ac/Ds

The *Ac* element is 4,565 bp in length with 11-bp terminal inverted repeats (TIR) (Federoff *et al.*, 1984). The *Ds* elements have 11-bp terminal inverted repeats but with variation in internal sequence and length (Doring *et al.*, 1984). Although the *Ac/Ds* system is used for transposon-tagging, this method is not widely used due to its relatively low forward mutation rate of 10^{-6}/gene/generation. The transposition of *Ac/Ds* is favored to transpose locally (Walbot, 2000). The *Waxy* gene is an example of a gene cloned successfully using *Ac/Ds* elements (Federoff *et al.*, 1983).

En/Spm

The *En/I* system was discovered by Peterson (1953). McClintock independently discovered this same transposable element system in 1954 and named it *Spm/*d*Spm* (McClintock, 1954). The *En* element is 8,287 bp long and has 13-bp terminal inverted repeats with the first 5 bp conserved (Masson *et al.*, 1991). The *En/Spm* element yields two major transcripts, *TnpA* which is 2.5 kb long identified as Mutator (M), and *TnpD* which is 6 kb long and identified as Suppressor (S). Excision from the genome cannot occur without the presence of both the TNPA and TNPD proteins (Grant *et al.*, 1990,

Frey *et al.*, 1990). The transposition of *En/Spm* occurs to linked sites. The mutation rate is 10^{-6}/gene/generation, similar to *Ac/Ds*. The *Opaque2* gene was successfully cloned with *En/Spm* (Schmidt *et al.*, 1987).

Mutator

The *Mutator* family of transposable elements was first described by Robertson (1978). The autonomous element of the *Mutator* family is *MuDR* (Qin *et al.*, 1991; James *et al.*, 1993). There are at least 250 non-autonomous *Mu* elements that fall into 5 major sub-clades - the canonicals Mu1 through Mu8, Mu10 (Mu10 and Mu11), Mu12A, Mu12B, and Mu12C (Lisch, 2002, Hunter, 2010). Although *Mutator* is a diverse family, the non-autonomous elements share conserved ~220-bp terminal inverted repeats (TIR) (Chandler *et al.*, 1986; Lisch, 2002). The first successfully cloned gene from *Mutator* is *Viviparous1* (*Vp1*) (McCarty *et al.*, 1989). *Mutator* is favored for transposon-tagging due to its relatively high forward mutation rate of 10^{-4}/gene/generation (Walbot, 2000).

MuDR elements consist of two genes, *mudrA*, which encodes a transposase, and *mudrB*, required for new insertion into the genome (Woodhouse *et al.*, 2006). For transposition to occur, the MURA protein encoded by *mudrA* binds to a specific 32-bp conserved region of *Mu* TIR and initiates a double strand break (Benito and Walbot, 1997). The mechanism for *Mu* transposition is similar to that of *Ac/Ds*, but excision of *Mu* produces a 9-bp direct repeat (Le *et al.*, 2000).

Based upon the high forward mutation rate of *Mutator*, the Uniform*Mu* population was generated as a resource for functional genomics in maize (McCarty *et al.*, 2005, Settles *et al.*, 2007). The Uniform*Mu* population was developed by introducing active Robertson's *Mutator* transposons into inbred line W22 via repeated backcrossing. The homogenous inbred line facilitates genotype and phenotype associations (McCarty *et*

al., 2005). Methods using *Mu*TAIL (Settles *et al.*, 2004) and *Mu*-454 (Eveland *et al.*, 2008) are used to generate libraries that contain *Mu*-flanking sequences. The flanking sequences can be used in co-segregation studies aimed at associating the presence of specific *Mu* insertions with the observed mutant phenotype.

Research Objectives

The mutants *mini-me* and *grass* were identified in the Uniform*Mu* population, grown as part of the Cell Wall Genomics project (Penning *et al.*, 2009). Both mutants are extreme dwarfs that reach a height of no more than 25 cm, and form multiple tillers. The mutants have small, and narrow leaves, lack a true stalk, and do not form functional floral structures, although the *mini-me* mutant has, under certain circumstances, been observed to produce a floral structure that contains both male and female characteristics, but that is not fertile.

The objectives of this research were to characterize the mutants phenotypically and to clone the causal gene(s). The hypotheses for this research are: 1) the *mini-me* and *grass* mutations are caused by *Mutator* insertions; 2) the *mini-me* and *grass* mutations are allelic; 3) the tillering phenotype is caused by a lack of suppression of axillary meristems.

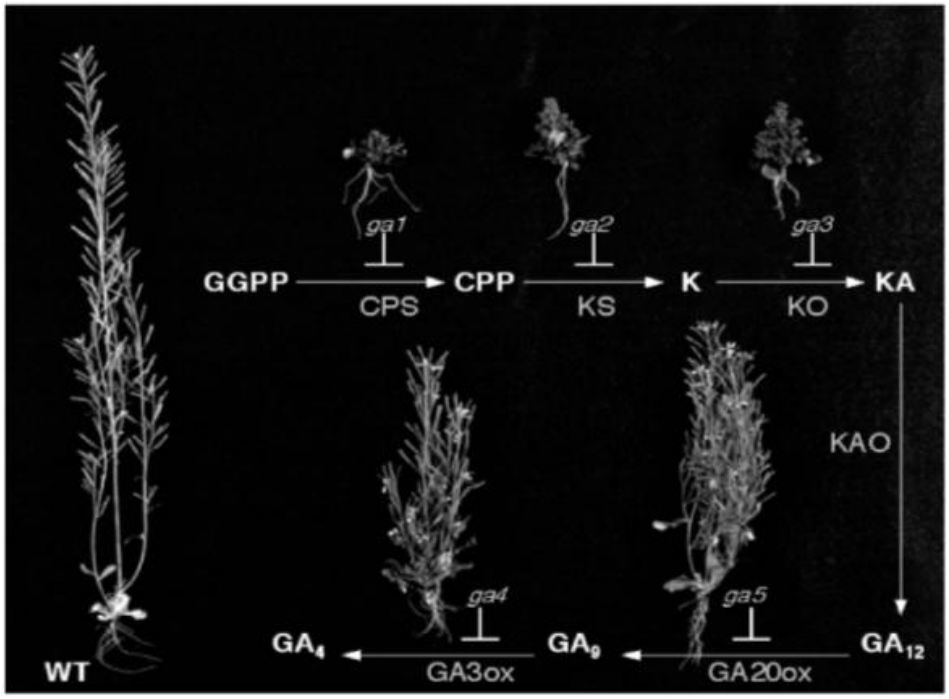

Figure 1-1. Known Arabidopsis dwarf mutants affecting the GA biosynthesis pathway. GGP: geranylgeranyl diphosphate, CPS: copalyl diphosphate synthase, CPP: cyclodiphosphate, KS: kaurene synthase, K: kaurene, KO: kaurene oxidase, KA: kaurenoic acid, KAO: kaurenoic acid oxidase, GA3ox: GA-3-oxidase, GA20ox: GA-20-oxidase. (Sponsel and Hedden, 2010)

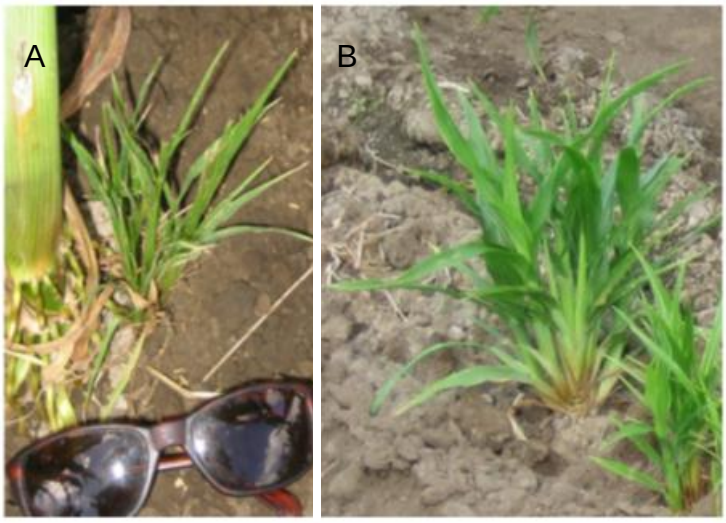

Figure 1-2. Phenotype of maize *grass* and *mini-me* mutants A) *grass*. B) *mini-me*. Photos taken by Wilfred Vermerris in the Puerto Rico 2005-2006 winter nursery.

CHAPTER 2
PHENOTYPIC CHARACTERIZATION OF THE *MINI-ME* AND *GRASS* MUTANTS

Introduction

As described in Chapter 1, the *mini-me* and *grass* mutants are extreme dwarfs with altered plant architecture: They do not grow more than 25 cm in height, lack a typical stalk typical, instead produce multiple tillers, and do not produce functional floral structures. The phenotype of both mutants varies depending on the environment as illustrated by the images of *mini-me* growing in the field in Puerto Rico (Figure 1-2) versus in a pot in the greenhouse at the University of Florida in Gainesville, Florida (Figure 2-3).

This chapter describes the morphological and anatomical characterization of both mutants to help identify the physiological basis of the phenotype. The initial focus has been on embryo morphology, seed germination, and leaf morphology, as outlined and justified below.

Variation in Embryo Structure

The meristem consists of undifferentiated cells from which the main organs develop. Above-ground organs form from the shoot-apical meristem (SAM), whereas the roots form from the root meristem. Since the SAM is ultimately responsible for forming the various above-ground organs, variations in plant architecture may be caused by abnormalities in the formation of the embryo itself, or by abnormalities in the way the embryo develops into a mature plant. Microscopic analysis of the embryo of wild type and mutant maize plants can address whether the basis for the altered architecture in the mutants is pre- or post-embryonic. In the case of post-embryonic

changes, it maybe possible to assess at which stage variation in architecture becomes apparent.

Variation in Seed Germination

Given the role of phytohormones on virtually all aspects of plant growth and development, chemical or spatio-temporal changes in phytohormones may manifest themselves as variation in the rate of seed germination.

Variation in Leaf Morphology

Small plant size can result from reduced cell size and reduced cell number. A comparison of epidermal peels of leaves from the mutant and wild-type plants viewed under the microscope can provide information on cell size, cell number as well as other morphological differences. Cross sections through the leaf blades can reveal additional changes in cell size and shape below the epidermis.

Materials and Methods

Plant Material

The sources for *mini-me* were S2008:234-S3 (“Summer 2008, row 234, selfed progeny of plant 3”), and S2008:234-S4, whereas the sources for *grass* were S2007:212-S2 and S2007:212-S4. The parental materials giving rise to these seed sources were known to be heterozygotes, and on average one quarter of these seeds resulted in plants displaying the mutant phenotype. The sources for wild-type inbred W22 were S2008:176-S6 and for inbred B73, S2008:370-S2 and S2008:370-S3. Seeds were germinated in a Jiffy seedling kit in the dark at 28˚C inside a Percival incubator. Once the seeds had germinated, the seedlings were transferred to the greenhouse with daylight length of 12 hours. For each experiment, 12 seeds per genotype were planted.

For the winter 2011 planting in the greenhouse at Gainesville, FL, the plants were grown in MetroMix 930 (BWI Companies, Inc.) under supplemental high-pressure sodium light (ACF Greenhouses, VA) to ensure 12 hours of light per-day.

Epidermal Peel

Abaxial and adaxial epidermal peels were prepared by covering a leaf section with clear nail hardener (New York Color, COTY Inc.). After the nail hardener dries out, it can be peeled from the leaves and mounted on a glass slide (Corning, Corning, NY). The imprints of the abaxial and adaxial leaf surfaces were viewed under the microscope. Freshly peeled abaxial and adaxial epidermal peels were stained with Toluidine Blue (Fisher Scientific, Waltham, MA). A commercial grid of 1x1 mm^2 (Sigma-Aldrich Co, St. Louis, MO) was used to calculate stomatal density.

Formalin-Acetic Acid-Alcohol (FAA) fixation

One liter of formalin-acetic acid-alcohol (FAA) for fixation of plant tissues was prepared by combining 850 ml 70% ethanol (Fisher Scientific, Waltham, MA), 100 ml 40% formaldehyde (Fisher Scientific, Waltham, MA) and 50 ml glacial acetic acid (Fisher Scientific, Waltham, MA) (Ruzin, 1999). After the plant material had been placed into FAA solution, it was vacuum infiltrated for faster penetration of the FAA solution into the plant cells and also to remove air bubbles. Leaf tissue was fixed for at least 24 hours, whereas harder plant tissues such as stem were incubated for 48 hours.

Infiltrating and Embedding Tissues- Paraffin/TBA method

After FAA fixation the tissue samples were dehydrated and infiltrated with the embedding agent paraffin to enable sectioning with a microtome. Since paraffin is an apolar compound, excess water must first be removed. This was achieved with a graded dehydration series in alcohol of increasing concentration. For each change,

harder plant tissues such as stems were left overnight, whereas for softer tissues such as leaves, 6 to 12 hours was sufficient (Ruzin *et al.*, 1999). *Tert*-Butanol (TBA) (Sigma-Aldrich Co, St. Louis, MO) is preferred for dehydration series (Cutler *et al.*, 2007). Once the plant tissues were in paraffin (Sigma-Aldrich Co, St. Louis, MO) at 56˚C, the plant tissues were left overnight so that TBA could evaporate and to allow paraffin to infiltrate the plant tissues.

Sectioning and Staining

Transfer of the tissue in the warm paraffin to ice solidified the paraffin, enabling sectioning with a rotary microtome (American Optical microtome model 820). The sections were mounted on Superfrost Plus Slides (Fisher Scientific, Waltham MA).

The Johansen method was used for staining: a combination of Safranin O (Sigma-Aldrich Co, St. Louis, MO) and Fast Green (Sigma-Aldrich Co, St. Louis, MO) (Johansen, 1940). This staining protocol is preferred because it yields brighter stains of plant tissues. Safranin O stained chromosomes, nuclei, lignified or cutinized cell walls red, while Fast Green stained cytoplasm and unlignified primary cell walls green. The working concentration for Safranin O was 1% in 2:1:1 methyl cellosolve (Sigma-Aldrich Co, St. Louis, MO): 95% ethanol: water. For Fast Green (Sigma-Aldrich Co, St. Louis, MO), the working concentration was 0.15% in 1:1:1 methyl cellosolve: 100% ethanol: clove oil (Sigma-Aldrich Co, St. Louis, MO) (Ruzin, 1999).

Microscopy

An MVX10 Olympus microscope located in the Forest Genomics lab (Cancer and Genetics Research Complex) was used to visualize and capture the images of the plant tissues after staining. The microscope was outfitted with an Olympus MVX-TV1XL digital camera.

Results

Variation in Seed Germination

Seeds from the selfed heterozygous *mini-me* plant S2008:234-S3 began to germinate after four days incubation in the dark at 28˚C (Figure 2-1-A). Of the twelve seeds three seeds were very slow to germinate 3 to 6 days after the W22 control seeds and siblings and were identified as putative mutants. Segregation of three mutant seeds out of seven is consistent with a 3:1 segregation ratio for a single recessive mutation (X^2 = 0.13, d.f.= 1 p=0.7150).

After eleven days (Figure 2-1-B) these putative mutant seedlings remained small relative to their siblings, but did not display any obvious differences in morphology. From a total of four trials or 48 seeds planted using the Jiffy seedling kit, only four *mini-me* mutants were obtained based on shorter plant height compared to the siblings. This is considerably fewer than the 12 *mini-me* mutants expected from a total of 48 seeds. This discrepancy is due to reduced viability of the mutants that led to premature death (Figure 2-1-B).

Seedlings from the selfed heterozygous *grass* plant (S2007:212-S2) also germinated more slowly (3-6 days later than W22) and showed variation in size (Figure 2-2), but no obvious differences in morphology were observed 13 days after planting (DAP). At 20 DAP however, some of the plants no longer elongated, and it became apparent that the leaves were growing opposite of each other (Figure 2-3-B), displaying a symmetry not observed in wild-type maize seedlings. In wild-type seedlings, subsequent leaves are positioned at an angle of approximately 140 degrees relative to the previous leaf. Three batches of 12 seeds were germinated. Due to arrested growth

in the early stages of germination or fungal infections a total of only three *grass* mutants were obtained (X^2 = 3.11, d.f.= 1, p=0.078).

The planting in the 2011 winter greenhouse at Gainesville, FL resulted in four *mini-me* mutants out of 10 seeds from S2008:234-S3 and two *grass* mutants out of 7 seeds from S2007:212-S2 (Figure 2-4). Two of the *mini-me* mutants produced floral structures with both male (tassel) and female (ear) characteristics (Figure 2-9). Pollen was sprinkled on the silks protruding from these floral structures, but seed formation did not occur based on visual inspection under a dissecting microscope 22 days after pollination (Figure 2-10).

Variation in Leaf Morphology

Leaf Blade Dimensions

The length and width of 12 *mini*-me and 8 *grass* leaves were measured. Twelve leaves of *mini-me* were measured to be on average 17 cm in length and 1.2 cm in width. For *grass*, the average length was 9 cm and 0.5 cm in width (Figure 2-5). The leaves of both mutants contained translucent sections. This is apparent from the images in Figure 2-6, which were taken with a light source underneath the leaf.

Epidermal Peel

In order to examine variation in cell patterning or morphology on the leaf surface, epidermal peels using clear nail hardener were prepared from nine *mini-me* mutant leaves from different plants (S2008-234-S3) and six *grass* leaves from different plants (S2007-212-S2) and analyzed under the microscope. One of each of the mutant samples was collected in between 2009 and 2011. Epidermal peels from phenotypically wild-type siblings of S2008:234-S3 and from inbred line W22 were used as controls (Figure 2-7). The frequency of stomata was lower for both mutants and the stomata had

irregular shapes compared to wild-type plants. Furthermore, the cell walls were irregular in shape and size that made counting of the cell files between stomata challenging.

The stomata density was calculated using an average of three random 1x1 mm^2 of the adaxial and abaxial leaf surfaces. A t-test showed that the stomatal density in the two mutants was statistically highly significantly different when compared to controls with control (Average, M = 48.33) and *mini-me* (M = 35.67), t(10.15) = 1.247, p = 0.0005. Also, control (M = 48.33) and *grass* (M = 28.0), t(8.994) = 2.26, p = 0.0008.

Cross Sections of the Leaf Blade and Midrib

The leaf cross section of the *mini-me* mutant from 2008-234-S3 (Figure 2-11-E) revealed irregular cell wall shape in all cells-epidermal cells, bundle sheaths, and vascular cells, when compared to the wild type (Figure 2-11-D). In addition, the bundle sheaths of the mutants were located closer next to each other and some were improperly formed compared to the control and also smaller in size compared to the wild type. The cross section of the *grass* leaf (Figure 2-11-F) looked overall similar to the *mini-me* mutant, but had an even more irregular epidermis on the adaxial side of the leaf, and the improperly formed bundle sheaths were more distinct (Figure 2-11-E). Both mutants (Figure 2-11-B, C) lack a distinct midrib when compared to the wild type (Figure 2-11-A).

Safranin O typically stains cutinized cells red typically at the epidermis and sclerenchyma as can be observed in wild type (Figure 2.11-D), but both mutants lack cutinized cells (Figure 2.11-E-F).

Cross section of the Meristems

The meristematic tissues of developing seedlings of one *grass* and three *mini-me* mutants were analyzed and compared to three wild-type controls (30 DAP and 20 DAP).

Due to the delay in development, it was challenging to obtain seedling tissues of identical developmental stages. All the seedlings contained a main shoot apical meristem (SAM) just below the leaf primordia. A secondary SAM was observed in the *mini-me* and *grass* seedlings (Figure 2-11-H-I).

Discussion

The *mini-me* and *grass* mutants share the extreme dwarf phenotype, they both lack of a main stem and midrib, and they both form tillers. Nonetheless, under field and greenhouse conditions the two mutants can be distinguished from each other because *grass* is smaller and has not ever been observed to produce floral structures. The detailed phenotypic characterization described above identified several additional similarities: slower germination rate, altered leaf morphology, both in terms of the number of stomata and epidermal cell shape and size, and the presence of an additional shoot apical meristem at the base of the main stem in the early seedling stage. These similarities in phenotype make it plausible that the two mutants are caused by defects in the same gene, but with slightly different impacts (penetrance).

The extra meristems in the mutants may reflect a premature development of vegetative axial meristems that in wild-type plants would ultimately give rise to ears (female flowers), but that in these mutants results mainly in the formation of tillers and occasionally may give rise to the feminized tassel in *mini-me*. The additional meristem could be caused by misexpression of an early homeodomain gene. Alternatively, the tillering in the two mutants could result from a lack of suppression of the axillary meristem as seen in *tb1* and *gt1*.

Both *mini-me* and *grass* had irregular cell shapes that were challenging to quantify. A close look at the irregularly shaped cell walls (Figure 2.12-B-C and 2.13-B-

C-D) suggests differences in cell differentiation. According to Moose *et al*. (1994), maize bulliform cells stain purple with Toluidine blue. As observed in the adaxial epidermis of *mini-me* and *grass* (Figure 2.8-B-C), the cells that are stained purple are uneven in size and distribution compared to the wild type control (Figure 2.8). This is further evidence of changes in cell differentiation. In addition, the bundle sheaths of both mutants were not clearly formed compared to the control (Figure 2.11-E-F).

The maize *tangled-1* (*tan-1)* (Smith *et al*., 1996) mutant was shown to have defects in both epidermis and bundle sheaths due to improper formation of the phragmoplast. Another maize mutant affected in epidermal cell differentiation is *discordia1* (*dcd1*). The functional *Dcd1* gene encodes a phosphatase involved in pre-prophase band (PPB) formation (Gallagher *et al*., 1999, Wright *et al*., 2009).

The *mini-me* floral structure is shaped like a tassel containing pseudo-ovaries with silks. This floral structure, however, appears to be infertile, because pollination with W22 pollen did not result in the formation of an embryo (Figure 2.10-C). Examples of similar mutants are *anther-ear1* (*an1*) and *nana1.* The *an1* mutant is short in stature with anthers present in the spikelet of the ear. This is the result of a defect in the GA-biosynthesis pathway (Bensen *et al*., 1995). The *nana1* mutant is also short and contains a feminized tassel due to a defect in the brassinosteroid biosynthesis pathway.

The mutants will likely be affected by a less efficient carbon dioxide uptake due to fewer stomata, which will lead to reduced photosynthetic activity. This could be the reason that most mutants do not live as long as normal maize plants: at most 90 days under extreme care with regular watering, fertilization, and avoidance of insect pests.

The similarities in phenotype make it plausible that the two mutants are caused by defects in the same gene, but with slightly different impacts (penetrance). There are many morphological and anatomical changes in the *grass* and *mini-me* mutants, that appear to be more complex than in other known maize mutants that resemble *mini-me* and *grass* in certain aspects, as described above and in Chapter 1. For example, *an1* and *nana1* have altered floral structures, but produce normal vegetative parts of the plant, *tb1* and *gt1* produce tillers, but are able to form normal flowers, and *br2* and *d8* are short, but still look like their wild-type counterparts in other aspects. Given that the SAM of *mini-me* and *grass* appears to be normal, the mutants must be lacking one or more key signals required for normal post-embryonic development, and that are involved in meristem development, cell differentiation and/or integration of hormone signaling.

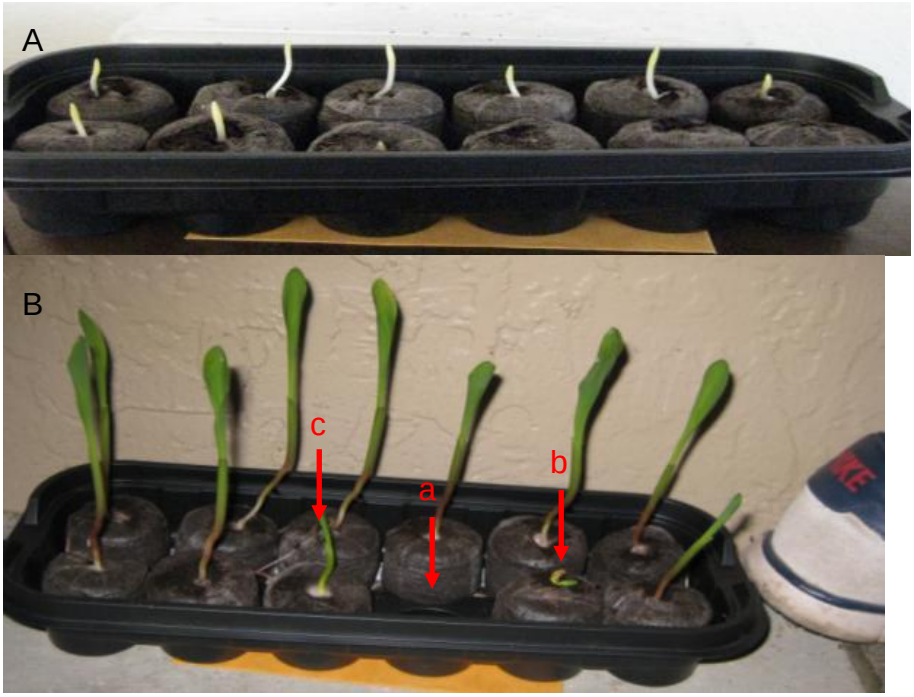

Figure 2-1. Seedlings growth. A) *Mini-me* (2008:234-S3) seedlings in the dark after 4 days in the incubator at 27°C**.** B) Family of seedlings segregating for *mini-me* (S2008:234-S3). c) Seedlings with a suspected mutant phenotype 11 days after planting. a) Seedlings removed due to fungal infection b) Seedling growth arrested.

Figure 2-2. A family segregating for *grass* (S2007:212-S2) 13 DAP with three putative mutant phenotype marked by red arrows.

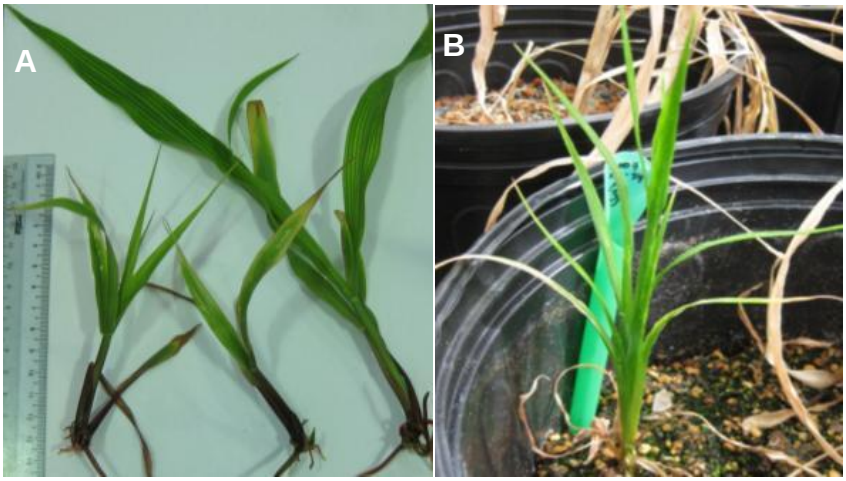

Figure 2-3. A) *Mini-me* (S20008:234-S3) showing the first two seedlings from the left are mutants and to the right is the wild-type/heterozygote plant 20 days after planting. B) *grass* (S2007:212-S4) showing leaves growing in opposites about 30 days after planting, May 2009.

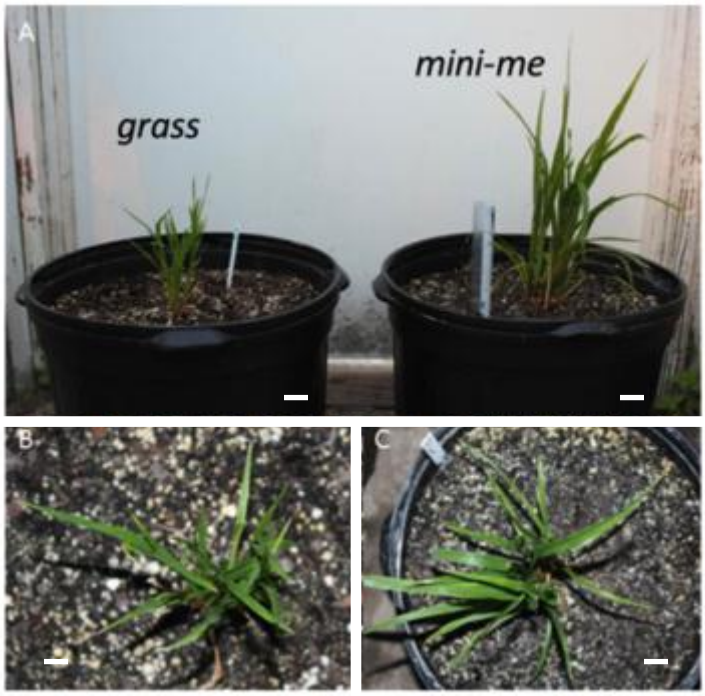

Figure 2-4. A) Front view of *mini-me* and *grass* grown in the winter greenhouse 2011, Gainesville, FL. B) top view of *grass*. C) top view of *mini-me*; scale bar represents 1cm

Figure 2-5. Comparison of leaf blade size of wild type (W22), *mini-me*, and *grass.*

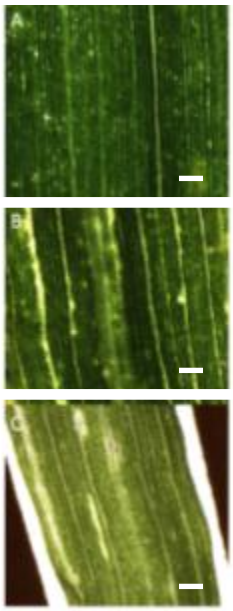

Figure 2-6. Translucent sections in the leaf blades of *mini-me* and *grass* mutants. Microscope images were acquired using a light source underneath the samples whereby the exposed sides were covered with black paper: A) Wild-type (W22), B) *mini-me*, C) *grass*, scale bar represents 100 µm.

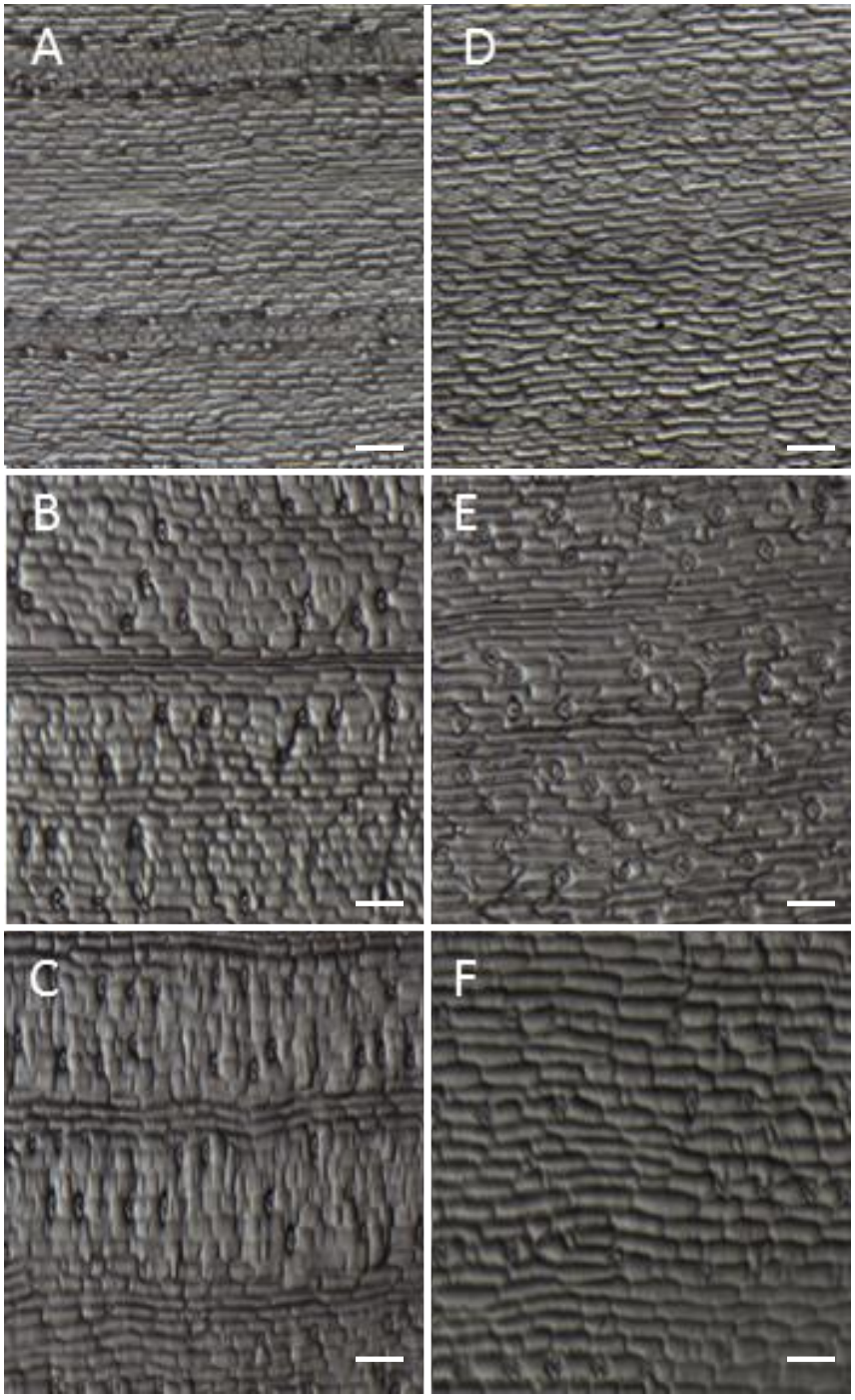

Figure 2-7. Epidermal imprints from leaf blades of wild-type, *mini-me,* and *grass* mutants. A) wild-type adaxial. B) *mini-me* adaxial. C) *grass* adaxial. D) wild-type abaxial. E) *mini-me* abaxial. F) *grass* abaxial; scale bar represents 10 µm.

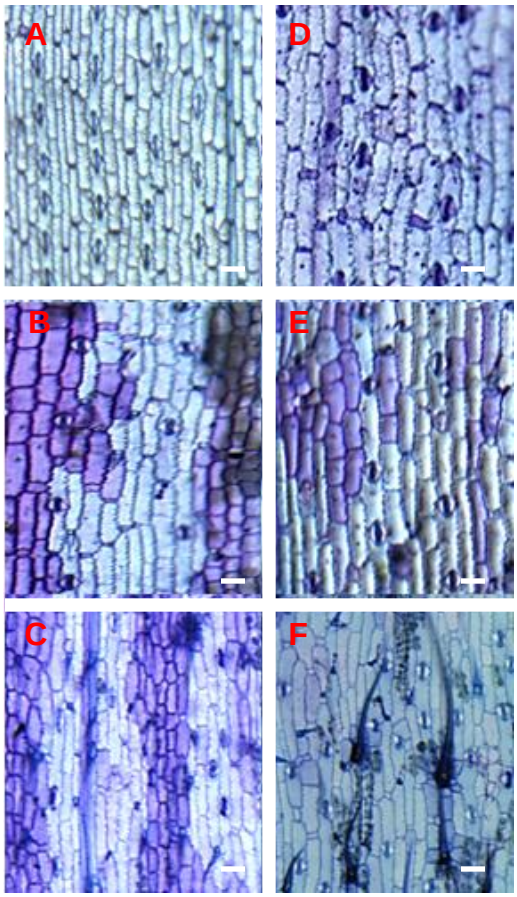

Figure 2-8. Epidermal imprints stained with Toluidine Blue from wild-type, *mini-me*, and *grass* mutants. A) wild-type adaxial. B) *mini-me* adaxial. C) *grass* adaxial. D) wild-type abaxial. E) *mini-me* abaxial. F) *grass* abaxial; scale bar represents 10 µm.

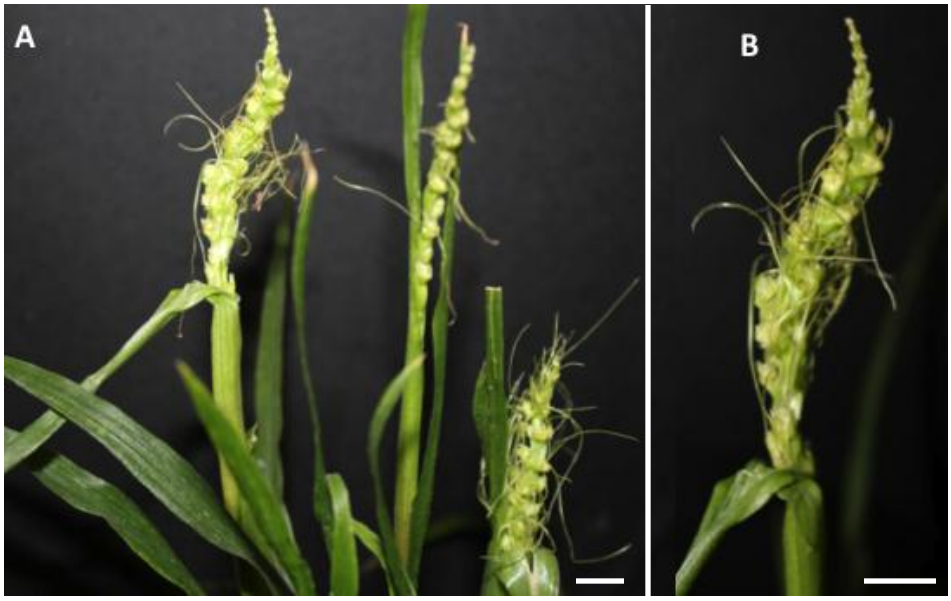

Figure 2-9. A) Flowering *mini-me* with three hybrid floral structures displaying both branchless male and female characteristics. B) Close-up of the hybrid floral structure; scale bar represents 1 cm.

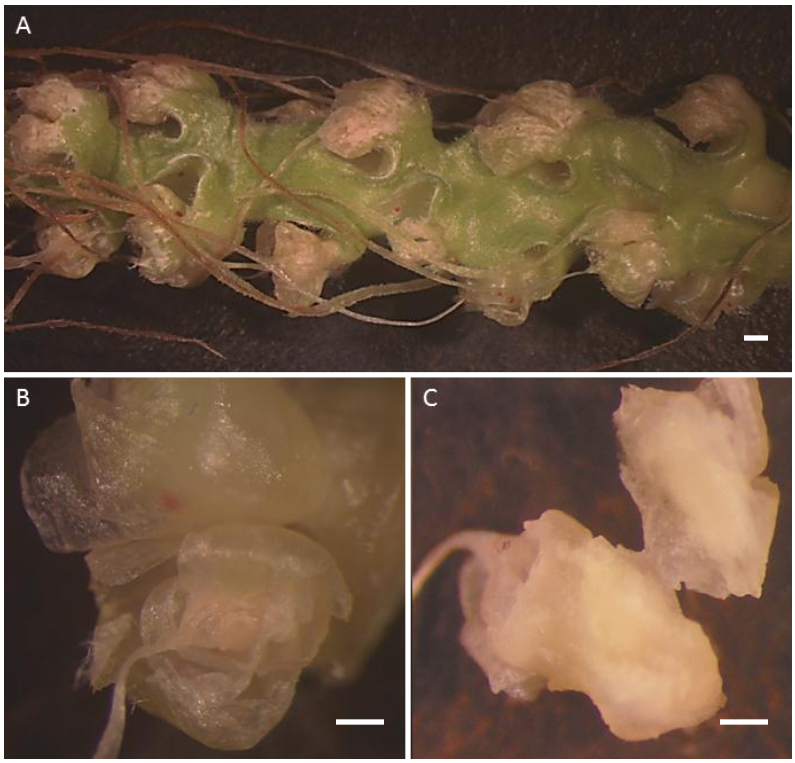

Figure 2-10. Floral structure of *mini-me*. A) Close up of the floral structure. B) Pseudo-ovary with silk (style). C) Pseudo-ovary sliced in half; scale bar represents 1 mm.

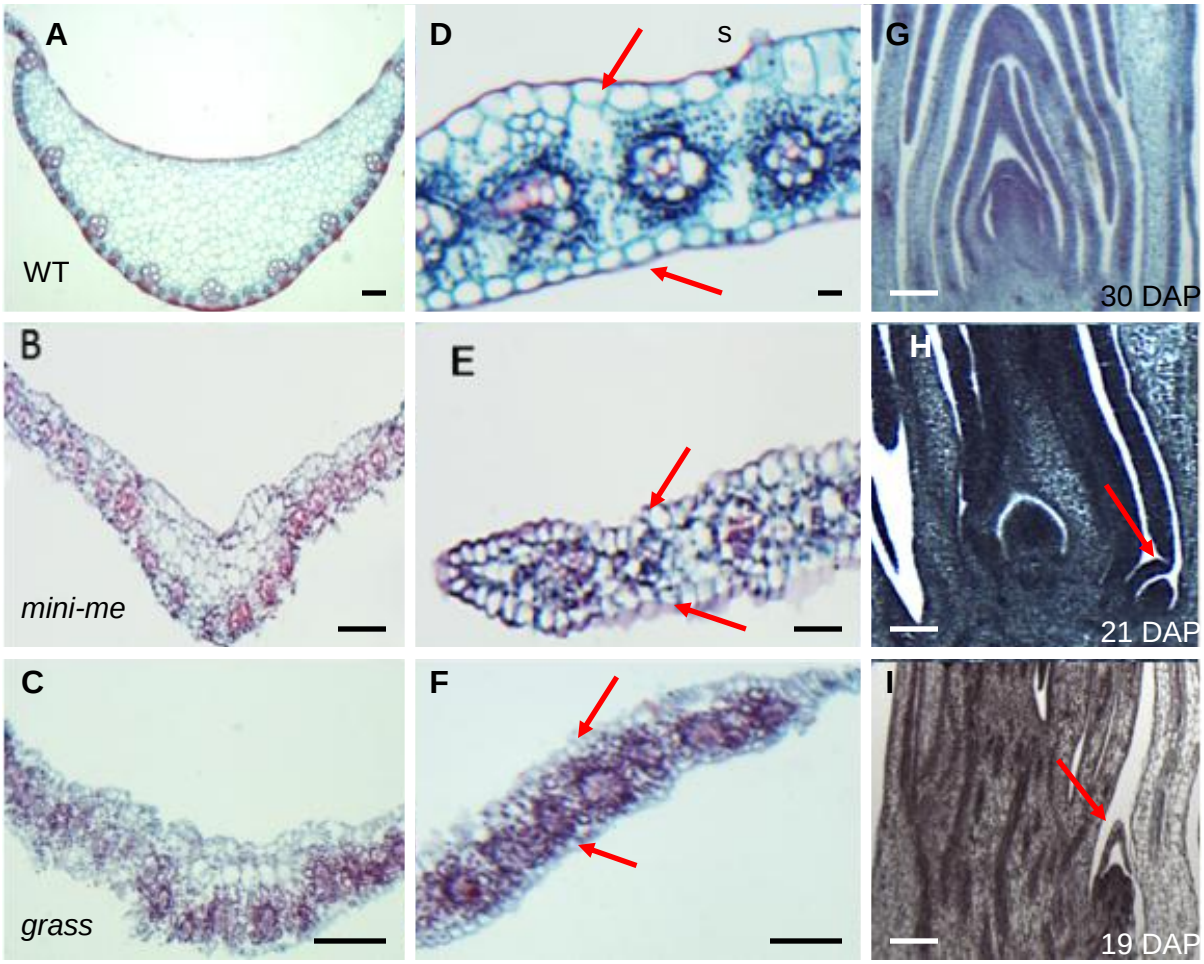

Figure 2-11. Cross section of midrib, leaf blade and meristem. Wild-type A, D, G. *mini-me* B, E, H. *grass* C, F, I. In D, E, F arrows showing upper and lower epidermis. In H, I arrow showing early differentiation of vegetative axial meristems. s-stoma; scale bar represents 100 µm.

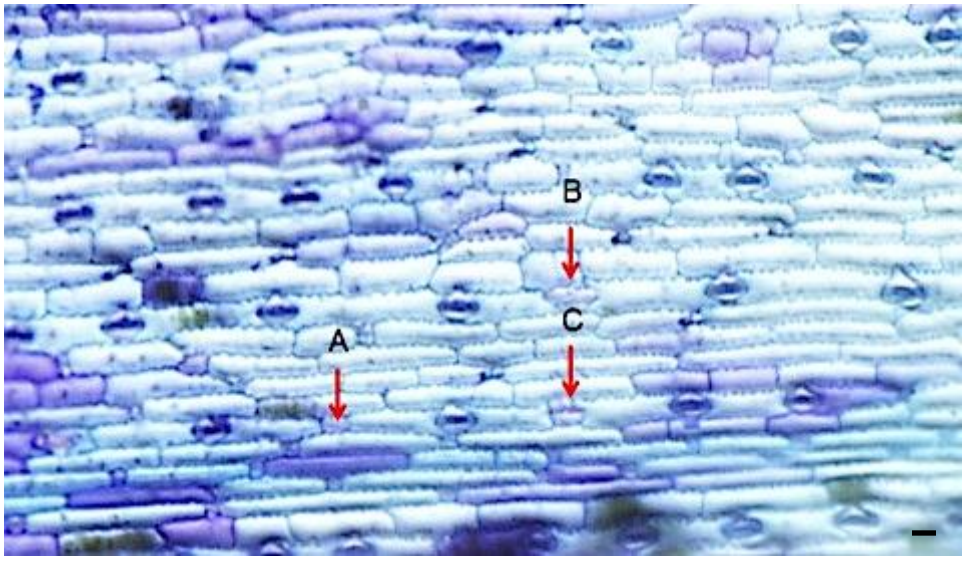

Figure 2-12. *mini-me* epidermal peel stained with Toluidine Blue. A) Putative guard cell pre-cursor. B and C incomplete stomatal differentiation; scale bar represents 10 µm.

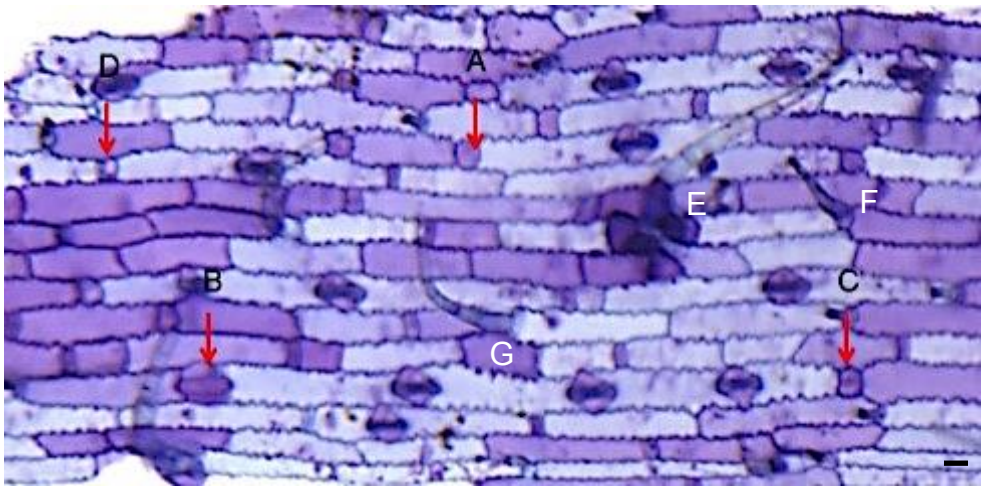

Figure 2-13. *grass* epidermal peel stained with Toluidine blue. A) Putative guard cell pre-cursor. B,C, and D incomplete stomatal differentiation. E) irregular macrohair patterning. F-G) irregular microhair; scale bar represents 10 µm.

Table 2-1. Stomatal density within 1x1 mm^2 in *mini-me, grass* and W22 leaf blades

	W22		*mini-me*		*grass*	
Replicate	Abaxial	Adaxial	Abaxial	Adaxial	Abaxial	Adaxial
1	48	34	37	22	29	20
2	50	35	36	18	24	21
3	47	36	34	24	31	19
Total	145	105	107	64	84	60
Average	48	35	35	21	28	20
Std. Deviation	1.5	1.0	1.5	3.1	3.6	1.0

CHAPTER 3
MOLECULAR GENETIC ANALYSIS AIMED AT CLONING THE *MINI-ME* AND *GRASS* GENES

Introduction

The *mini-me* and *grass* mutants were identified in the Uniform*Mu* population, grown as part of the NSF-funded Cell Wall Genomics project (Penning *et al.*, 2009). These mutant phenotypes were inherited as single recessive mutations based on the 3 wild-type: 1 mutant segregation ratio observed when the progeny of selfed heterozygotes were planted. As described in Chapter 2, *grass* and *mini-me* have very similar phenotypes and may be allelic.

Given that the mutants were identified in the Uniform*Mu* population, the cause of both mutations was likely *Mutator* insertions, although spontaneous mutations can never be ruled out. In order to identify the *Mutator* insertion responsible for the mutant phenotype, a co-segregation analysis was carried out. The principle of a co-segregation analysis is the identification of a *Mutator* element that co-segregates with the mutant phenotype, i.e. that is present in all of the mutants while absent in all of the homozygous wild-type siblings (Figure 3-1, 3-2). Several methods exist to identify a co-segregating *Mutator* element. In the analysis described in this chapter, two high-throughput methods were used: *Mu*-TAIL PCR (TAIL- Thermal Asymmetric InterLaced) (Liu *et al.*, 1995, and Settles *et al.*, 2004) and *Mu*-454 (Eveland *et al.*, 2008). The principle of *Mu*TAIL is to generate a library of DNA fragments flanking the *Mu* insertion by using the *Mu* TIR sequences as an anchor on one end and an arbitrary primer that anneals to the flanking DNA within amplifiable distance at the other end. The *Mu*-454 approach is based on the 454-high-throughput sequencing platform (Margulies at al., 2005), with the same

objective as *Mu*-TAIL, namely to generate a library of *Mu* flanking sequences. In principle the *Mu*-454 method has better coverage of the genome, is less laborious, faster, and offers higher throughput. Identifying the *Mutator* element causing the mutation can be complicated by the fact that *Mutator* is a high-copy number transposon. The identification of a map location of the mutation, combined with the map location of the individual *Mutator* elements identified with the high-throughput sequencing analyses can help narrow down the number of candidate *Mu* elements. Mapping the mutation can be accomplished in a segregating F2 population derived from a cross between the mutant (or heterozygote) and a genetically different inbred line. Being a member of the Iowa Stiff Stalk Synthetics, inbred B73 represents a different heterotic group than W22, which belongs to the Lancaster Sure Crop group.

There are two approaches to identify if *mini-me* and *grass* are alleles of the same locus. The classic genetic approach is to cross the two mutants and show that the progeny display the mutant phenotype. This approach is complicated by the fact that both mutants are sterile and cannot be crossed directly. As a consequence, it is necessary to cross two heterozygotes, each containing one of the mutant alleles, with each other. The concept of this approach is displayed in Figures 3-4 and 3-5. A molecular approach that could be used as preliminary evidence for allelism is to show that both mutants contain a mutation in the same gene, and that this mutation co-segregates with the mutant phenotype in both mutants.

Materials and methods

DNA Extraction

Plant DNA was extracted from frozen leaf tissue kept at -80˚C. DNA was extracted using the DNeasy Plant Mini kit (Qiagen, Carlsbad, CA). The DNA was stored at -20˚C.

Plant Material

For co-segregation analysis the following genotypes were used for *mini-me*: S2008:234-S3 and S2008:234-S4 (Summer 2008, row 234, selfed progeny of plant 3 and plant 4; mutants) and W22 (wild-type). Both sources represent progeny from self-pollinated heterozygotes so that homozygous mutants are expected among the progeny. As wild-type siblings, progeny from S2008: 234-S5 was used. This line was selected because all progeny had wild-type phenotypes, indicating that the parent was a homozygous wild-type sibling of heterozygous plant S2008-234-S3 and S2008-234-S4. For *grass*, the following sources were used: S2007:212-S2 and S2007:212-S4 (mutants). The wild-type sibling for *grass* was S2007:212-S1.

A mapping population was generated to be able to map the *mini-me* and *grass* loci. The following crosses were made in the Puerto Rico 2009 winter nursery: S2008:234-S3 and S2008:234-S4 (mutants) with B73 (female wild-type). For *grass*, the following genotypes were used: S2007:212-S2 and S2007:212-S4 (mutants) and B73 (female wild-type). The F1 progeny of *grass* and *mini-me* from Puerto Rico were self-pollinated in the summer 2010 Live Oak nursery to generate F2 seeds.

Due to poor seed set these crosses were repeated in the summer 2010 nursery in Live Oak, FL. Additional mapping populations for *mini-me* and *grass* were created in the 2011 winter greenhouse in Gainesville, FL. The genotypes that were used were *mini-me* (S2008:234-S3) and *grass* (S2007:212-S2) with B73 as the wild-type.

Backcrosses were done with W22 as female with heterozygotes of *mini-me* (S2008-234-S3) and *grass* (S2007-212-S2) to reduce *Mu* insertions.

*Mu*TAIL

The *Mu*-flank sequences for *mini-me* obtained via *Mu*-TAIL PCR (kindly provided by the Koch and McCarty Labs) were compared first to a library of *Mu* elements from the progenitors of the mutants in an attempt to identify unique *Mu*-flank sequences in the mutants that could be responsible for the mutations. The resulting 71 *Mu* insertions were then placed on the maize genome by performing a BLAST search of the flanking sequence against the maize genome (http://www.maizesequence.org; Schnable *et al.*, 2009).

Mu-454 Sequencing

One mutant each from *mini-me* (S2008:234-S3) and *grass* (S2007:212-S1) were used to prepare *Mu*-454 libraries. First, the DNA of each mutant was sheared at the ICBR core facility, resulting in many DNA fragments, some of which contained *Mu* inserts. A biotinylated B-adaptor was ligated to the sheared DNA, and fragments containing B-adaptor were captured with a streptavidin-magnetic bead and a magnetic rack. The primer TIR6, recognizing the TIR of *Mu* elements, was used in a primer extension reaction to make a DNA copy of those fragments containing the TIR of a *Mu* element. After melting the dsDNA and removal of the template strand with a magnetic bead, the newly synthesized strand served as a template for PCR using a biotinylated B-adapter primer and nested primer TIR8. After size selection streptavidin beads were mixed with the amplified sequences. The biotinylated strand was captured after the dsDNA had been melted in an alkaline solution. A second primer extension reaction with a TDA primer containing an A-adaptor, a 4-base variant library identifier, and a nested *Mu* TIR primer, was carried out. After removal of the template strand using the streptavidin magnetic beads, the *Mu*-library was ready for 454 sequencing, relying on

the B-adapter for annealing to a bead and using the A-adapter as the target for the sequencing primer. Unique sequences were identified with the clustering method from different libraries classified as parents (McCarty *et al.*, 2005)

Co-segregation Analysis

PCR was used to amplify genomic DNA fragments of candidate genes. A typical reaction contained per 25 µL: 10 ng genomic DNA, and REDTaq ReadyMix PCR Reaction Mix with $MgCl_2$ (Sigma-Aldrich Co, St. Louis, MO). A three-step PCR program was used consisting of 94˚C for 40 s for denaturation, 60˚C for 30 s for annealing, and 72˚C for 40 s for extension with 35 cycles and final extension of 2 min at 72˚C with a C-1000 thermal cycler (Bio-Rad Laboratories Inc., Hercules, CA)

Gene-specific primers (GSP) for unique *Mu*-flank sequences identified via *Mu*-TAIL PCR of *Mu*-454 were designed with Oligo v.6.8 software, followed by PCR product analysis on agarose gel (Fig 3-2). The objective was to identify *Mu*-flanking sequences that co-segregated with the mutant phenotype. Primers that annealed to genomic DNA on the other side of the *Mu* element could be designed based on the maize genome sequence database (http://www.maizesequence.org).

SSR Analysis

DNA from the 25 F2 *grass* mutants (obtained from a population of 120 grown in greenhouse individuals) was extracted and pooled and used in a mapping experiment conducted in the Settles lab. The PCR contained 0.25 µM SSR primers, 150 µM each dNTP, ~40 ng DNA, and GoTaq® PCR mix (Promega Co., Madison, WI). A PCR program was used consisting of 34 cycles of denaturation 94°C for 40 s, annealing at 57°C for 45 s, and extension at 72°C. The SSR primers used in this experiment amplified sequences known to be polymorphic between B73 and W22 (Martin *et al.*,

2010). In order to confirm if the parental alleles were segregating as would be expected for an F2 population, an SSR marker in an unknown location near the ZmARF7 gene (Xing et al., 2011) was used to test for segregation

Allelism Test

In order to conduct an allelism test to determine whether *mini-me* and *grass* are alleles of the same locus, phenotypically wild-type plants obtained from selfing a *mini-me* heterozygote were crossed with phenotypically wild-type plants obtained from selfing a *grass* mutant. In winter 2011, due to limited seed supplies, pollen from phenotypically wild-type plants was collected and used to pollinate six phenotypically wild type plants from the *mini-me* population. In addition, the male parents were self pollinated.

To identify allelism based on the sequence data, a search was performed for *Mu*-flank sequences obtained from the two mutants that mapped to the same locus. A co-segregation analysis as described above was subsequently used to identify putative causal mutations.

Results

Molecular Analysis of Flanking Sequences Identifed with *Mu*TAIL and *Mu*-454

For *mini-me* a total of 71 sequences were obtained from *Mu*TAIL and 10 unique sequences from *Mu*-454 (Table 3-1). None of the 10 sequences overlapped with the 71 *Mu*TAIL sequences.

For *grass*, 29 unique sequences were obtained from *Mu*-454 (Table 3-1); the *Mu*-TAIL analysis was not performed for this mutant. All sequences were mapped to the maize genome (Table 3-1). Initially co-segregation analysis was performed starting with chromosome 1. Not all primer pairs generated products, which may reflect strong

secondary structures in the DNA and/or high GC-content. Of 81 primer pairs tested for *mini-me*, 50 generated products, but none of the products co-segregated with the mutant phenotype (Table 3-1).

For *grass*, 15 of 29 primer pairs resulted in products, but none of the products co-segregated (Table 3-1).

Mapping Population

The yield from 2009 Puerto Rico winter nursery where the F2 mapping population was initiated was very poor. For *mini-me* only 40 F1 kernels were obtained, whereas 70 F1 kernels were obtained from the cross with the *grass* mutant.

The F1 progenies from Puerto Rico 2009 were planted in the 2010 summer nursery in Live Oak, FL. The *mini-me* F1 progenies succumbed to larvae, but the *grass* F1 progenies were advanced to the F2 generation. A total of 120 F2 seeds were planted in the greenhouse and yielded 25 mutants, consistent with the expected number assuming that the *grass* mutation is inherited as a single recessive allele (X_2 = 1.11, d.f.= 1; p=0.29,). The SNP mapping in the Settles lab pointed to enrichment on chromosome 10.

The crosses that were repeated at the winter 2011 greenhouse at Gainesville, FL, were grown based on six out of ten phenotypically wild type plants from the *mini-me* population to B73 and four (out of seven) phenotypically wild type plants from the *grass* population to B73.

SSR Analysis

DNA from 25 F2 *grass* mutants was pooled. DNA polymorphisms between the pooled DNA from these mutants and B73 identified with a set of SSR markers were analyzed (Martin *et al.*, 2010) in the Settles lab by Frederico Martin. The assumption is

that all mutants contain the W22 allele near the mutant locus, whereas at all other loci they will contain either the W22 or the B73 allele, or both (in case of heterozygotes). With bulk segregant analysis (BSA) of the pooled mutants, the results pointed to enrichment on chromosome 3L (SSR marker umc1528). When the mutants were tested individually for the marker allele at this locus, however, there was no apparent linkage between umc1148 and the mutant phenotype. There were 6 individuals homozygous for the B73 allele, 7 homozygous for the W22 allele, and 12 heterozygotes, consistent with a 1:2:1 segregation expected in the absence of linkage (X_2 = 3.84, d.f.= 2, p=0.147).

As the putative map location on chromosome 3L was investigated, the *embryo9* (*emb9*) locus (Clark and Sheridan,1991), which maps on chromosome 3L, was considered as a candidate (Neuffer,1993). The *emb9* mutant produces an enlarged embryo that cannot develop into a seedling, possibly due to a hormone defect. Some of the seeds in the segregating *mini-me* families S2008-234-S3 and S2008-234-S2 were phenotypically similar to *emb9* seeds. The *emb9* phenotype was observed after the experiments that showed the variation in germination of the seedlings. Since a mutation of the *emb9* locus would explain the reduced germination rate the hypothesis was formulated that the *mini-me* and *grass* mutants contain weak *emb9* alleles, i.e. the penetrance of the mutation is not complete, allowing some seedlings to germinate. The presence of tillers and reduced height in the mutants is consistent with a hormone defect, especially auxin. This hypothesis gained further support since the map location for the one *Mu* insertion identified with Mu-454 that was common in both *grass* and *mini-me* was located in Zm*ARF10* (Liu et al., 2009), encoding an auxin response factor. The specific location of this shared fragment on chromosome 3 was between

155,263,627 and 155,263,776 bp. The insertion site was 1 base pair apart in the two mutants. A co-segregation analysis using gene-specific primers for this gene yielded products in both mutants and wild-type siblings, suggesting that the insertion in the Zm*ARF10* gene was not responsible for the *mini-me* or *grass* phenotype. In combination with the fact that the insertions were 1 bp apart in the two mutants, this insertion was likely present in the progenitor.

Two *Mu* insertions in Zm*ARF10* were identified in the UniformMu database (http://uniformmu.uf-genome.org/): UFMu1449 and UFMu3476. The seeds from the two lines were obtained from the Maize Genetics Stock Center in Champaign-Urbana, IL and grown in the 2011 winter greenhouse, Gainesville, FL. The seeds germinated, and no apparent mutant phenotype was observed in the plants. The plants were self-pollinated to maintain the stock.

Two additional SSR markers located near Zm*ARF7* and Zm*ARF9*, both on chromosome 3 (Xing et al., 2011), were used to test for linkage to the *grass* locus. There was no polymorphism between W22 and B73 for the SSR marker near Zm*ARF9*. The SSR marker near *ZmARF7* was polymorphic, but there was no evidence for linkage to the *grass* locus in the F2 population. There were 5 individuals homozygous for the B73 allele, 7 homozygous for the W22 allele, and 11 heterozygotes, consistent with a 1:2:1 segregation expected in the absence of linkage (X^2 = 3.84, d.f.= 2, p=0.147).

In summary, there was no evidence to support a map location for *grass* on chromosome 3, nor for an involvement of Zm*ARF* candidate genes on this chromosome.

SNP Analysis

Based on SNP analysis (Liu *et al.*, 2009) of pooled *grass* samples in the Settles lab, there was a strong enrichment for the W22 allele on chromosome 10, spanning a 56 Mbp region (AGPv2 84-140 Mbp). There are three *Mu* insertions on chromosome 10 that could either be responsible for the grass phenotype, or, given the possibility that not all *Mu* insertions were captured, that may show linkage to the mutation. In the latter case the 56 Mbp region could be narrowed down. None of the three *Mu* insertions co-segregated with the mutant phenotype, ruling out their involvement in causing the mutation in the F2 *grass* population.

Analysis of the 25 *grass* mutants in the F2 population showed that all plants were homozygous wild type at the *Mu* insertion sites from chromosome 10, because PCR amplification with gene-specific primers generated a product, whereas amplification with a gene-specific primer and a *Mu*-TIR primer did not. Homozygosity for wild-type alleles at these loci can be explained by the *Mu* insertions are unlinked to the grass phenotype. Also, if the heterozygous plant containing the Mu insertion is crossed to B73 and only the wild type allele from the heterozygote plant is inherited in the F1, only the wild type allele will be produced in the F2.

In addition, based on the putative enrichment in the mutants for a region of chromosome 10, an SSR marker near Zm*ARF28* was tested based on Xing *et al*. (2011). This marker was not polymorphic between B73 and W22.

Allelism Test

The seven seeds from the segregating *grass* population planted in the winter 2011 greenhouse produced four phenotypically wild-type plants, whereas the 10 seeds from the segregating *mini-me* population resulted in six phenotypically wild-type plants, five

of which produced fertile ears. In order to maximize the ability to detect mutants from the allelism test of *mini-me* and *grass*, pollen from the normal *grass* siblings was pooled and pollinated onto the ears from the phenotypically wild-type plants in the *mini-me* population (Figure 3-4). Pollinating ears with pooled pollen increased the probability of crossing two heterozygotes. The probability that there was at least one heterozygote among the four male plants was 0.988 (calculated as 1-probability that all four males were homozygous wild type = $1 – (1/3)^4$). This effectively guarantees that a heterozygous *mini-me* ear receives some pollen carrying the *grass* mutant allele. In contrast, without pooling, the probability that a heterozygous *mini-me* ear would be pollinated by a heterozygous *grass* plant would be 2/3 (0.67). With so few plants, there is a real possibility that by chance all *mini-me* heterozygotes would be pollinated by wild type males from the *grass* population.

Discussion

A very large number of unique *Mu* flanking sequences was identified in *mini-me* with *Mu*-TAIL (71 sequences), whereas a much smaller number of sequences was identified with 454-*Mu* (10 sequences). Since the 10 sequences obtained from 454-*Mu* did not show overlap with the library obtained from *Mu*-TAIL this indicate technical problems (poor DNA quantification, poor library, poor sequencing data) with the 454-*Mu* procedure. It also suggests an even larger number of *Mu* insertions may exist than the 71 identified with *Mu*-TAIL since typically 20-30 unique *Mu* insertions are expected, the *mini-me* mutant represents an unusual situation.

The *Mu*-454 data for *grass* are more typical (30 insertions), but this may not represent complete coverage either, given the *mini-me* results. *Mu*-TAIL and *Mu*-454 library did not work out. A similar approach had been used to identify a candidate gene

underlying a different mutation in the Uniform*Mu* population, but also without success (Tayengwa, 2008, thesis). Based on these experiences, the depth of coverage with these methods may not be adequate. Indeed, according to Settles *et al*. (2004) only 67%-86% of the known *Mu* inserts were identified with the Mu-TAIL procedure. Hence, it is likely that not all *Mu*-insertions from *mini-me* and *grass* were sequenced.

The chromosome 3 location was identified in both *mini-me* and *grass* with the *Mu*-454 data. The Zm*ARF* genes are transcription factors that bind to early auxin response genes (Tiwari et al., 2003) and would be a good candidate gene given the role of auxin in suppressing axillary meristems but the co-segregation analysis did not confirm the role of this gene as a potential candidate.

The three *Mu* insertions identified on chromosome 10 did not co-segregate with the mutant phenotype. Instead wild type alleles were amplified in all mutants and controls indicated that these three insertions are not responsible for the mutant phenotype or the heterozygote parent of the insertion is not associated with the mutant phenotype. A probable explanation for generating wild type alleles in the *grass* F2 population is that the *Mu* insertions are unlinked to the *grass* phenotype. Also, if the heterozygote plant containing the *Mu* insertion is crossed to B73 and only the wild type allele is inherited in the F1, only the wild type allele will be present in the F2.

Despite the lack of clear support for linkage between the mutant phenotype and *Mu*-insertions in Zm*ARF10* and on chromosome 10, these candidate loci cannot be completely ruled out as a result of inherent challenges with PCR. The inclusion of positive and negative controls would be able to take away some of this uncertainty.

There could be a possibility that the candidates Zm*ARF10* and the three *Mu* insertions from chromosome 10 could be the candidate gene. Alternative methods could be devised to re-analyzed the candidate genes that includes a positive and a negative PCR control.

As for the allelism test conducted in the winter 2011 greenhouse, the two mutants will be considered allelic if mutants are the same phenotype is observed in the progenies of *grass* and *mini-me* crosses. Verification as to whether the *grass* allele is segregating in the progenies can be obtained based on phenotypic characterization of seedlings originating from selfed *grass* seeds. Lack of mutant plants in the progenies from the allelism test could be the result of an absence of the mutant *mini-me* allele (all parents were homozygous wild type by chance), or progeny sizes that are too small to observed mutants, given that the pooling strategy employed may reduce the frequency of the mutant alleles.

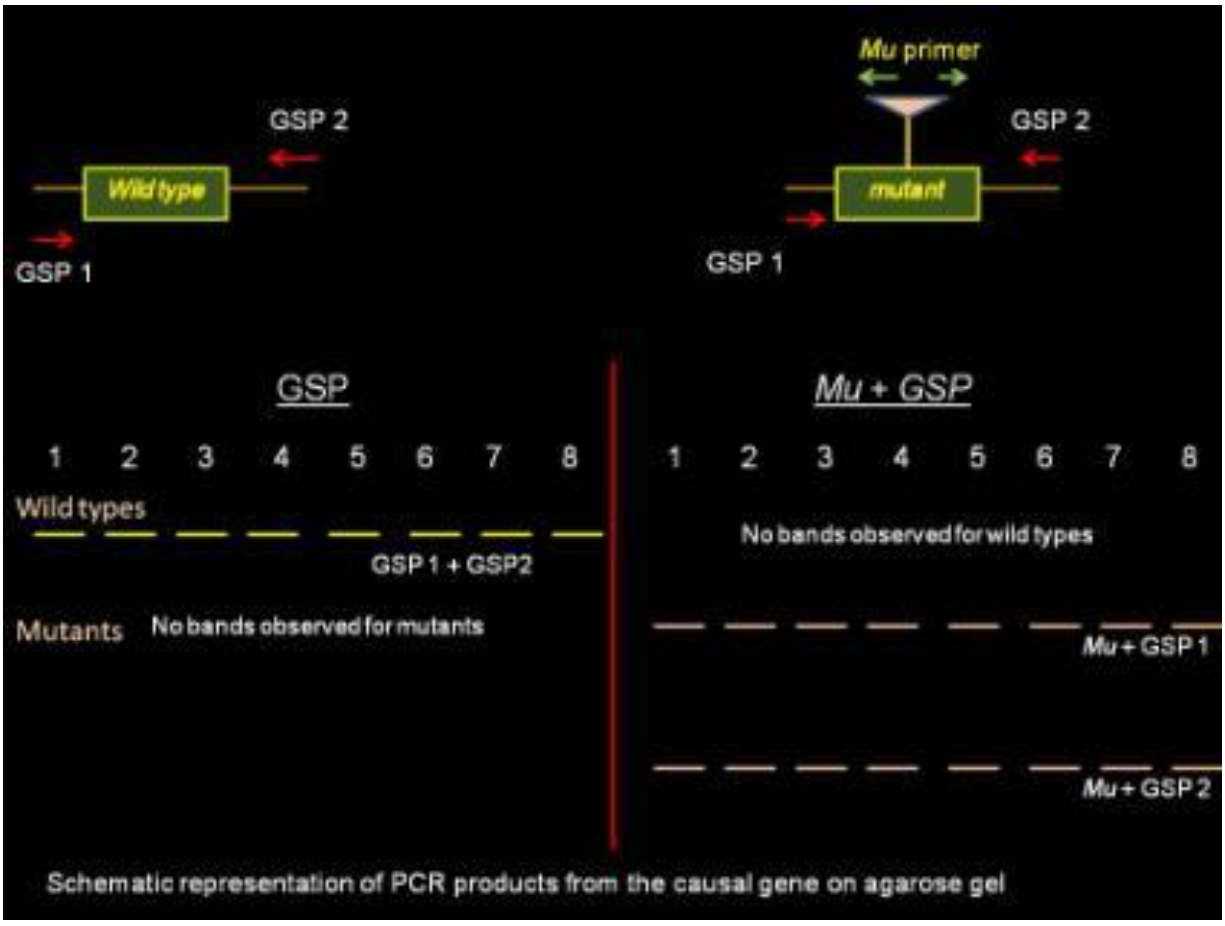

Figure 3-1. Schematic representation of the expected result when the *Mu* insertion and the mutant phenotype co-segregate

P B73 x heterozygous (*mini-me/grass*)

↓

F_1 (self)

↓

F_2 (for mapping)

Figure 3-2. Mapping population of *mini-me* and *grass*

		Ear (female)	Ear (female)
		1/3 *grass* WT	2/3 *grass* HET
Tassel (male)	1/3 *mini-me* WT	1/9	2/9
Tassel (male)	2/3 *mini-me* HET	1/9	4/9

Figure 3-3. Schematic representation of the procedure to make the allelism cross between *grass* and *mini-me*, and the expected outcome

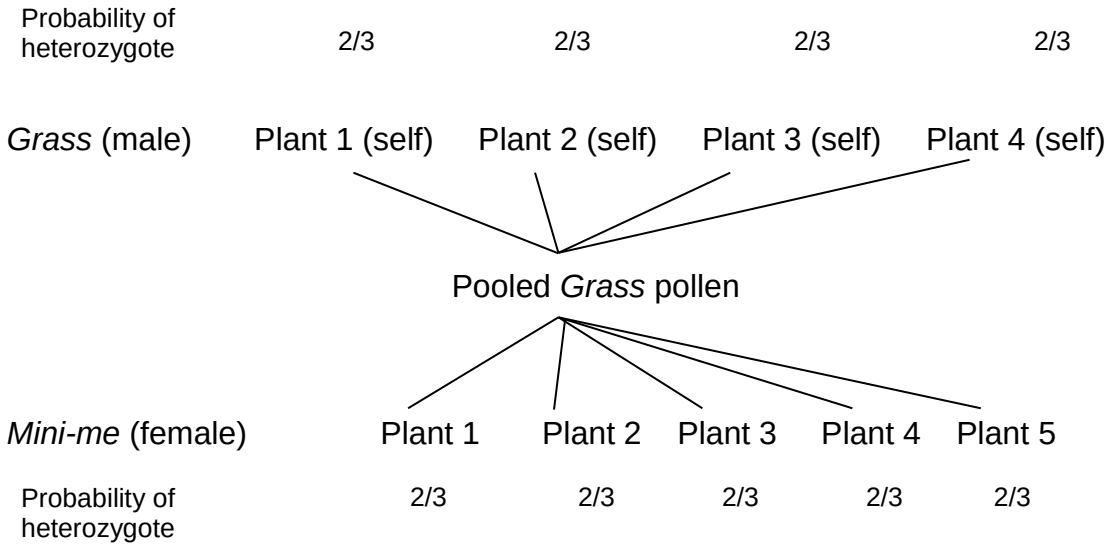

Figure 3-4. Schematic representation of the allelism cross in the winter 2011 greenhouse, Gainesville, FL

Table 3-1. Number of flanking sequence in each chromosome and primers that were tested

	Mini-me			*Grass*	
Chromosome	*Mu*-TAIL	*Mu*-454	Successful amplification	*Mu*-454	Successful amplification
1	10	1	8	0	0
2	15	0	11	7	4
3	11	3	9	2	1
4	8	1	6	1	0
5	4	1	1	1	0
6	1	1	1	6	3
7	4	0	2	2	1
8	7	0	5	1	1
9	7	0	6	1	0
10	4	3	1	6	5
Unknown	0	0	0	1	0
Total	71	10	50	30	15

Table 3-2. *mini-me* and *grass* for 2011 winter greenhouse, Gainesville, FL with the numbers designating plant number

Label	Name	Phenotype	Selfed	Ear(W22)	Ear (B73)	Pollen
S2008-234-S3 1	*Mini-me*	Normal	no		30	
2	*Mini-me*	Normal	no		31	G 11,12,15,16
3	*Mini-me*	Normal	no		43	G 11,12,15,16
4	*Mini-me*	mutant				
5	*Mini-me*	Normal	no	17	29	G 11,12,15,16
6	*Mini-me*	mutant				
7	*Mini-me*	Normal	no		28	G 11,12,15,16
8	*Mini-me*	mutant				
9	*Mini-me*	mutant				
10	*Mini-me*	Normal	no		40	G 11,12,15,16
S2007-212-S2 11	*Grass*	Normal	no	26	35	
12	*Grass*	Normal	yes		32,41	
13	*Grass*	mutant				
14	*Grass*	mutant				
15	*Grass*	Normal	yes		45	
16	*Grass*	Normal	yes	23	27,34,36	

CHAPTER 4
DISCUSSION AND RECOMMENDATIONS FOR FUTURE WORK

The morphological analysis indicated that the tillering was caused by the initiation of an axillary meristem. This axillary meristem appears to be initiated as part of the post-embryonic development. The appearance of tillering may be due to changes in the synthesis or perception of one or more hormones that are known to suppress branching, such as auxin and strigolactone. Arabidopsis branching mutants are defective in hormone biosynthesis or signaling, but cross section analysis of the mutant meristems was not carried out (Sorefan *et* al., 2003, Schwartz et al., 2004, Zou *et al*., 2006), so that it is difficult to use the morphologic changes as evidence for the deficiency in a hormone. Another possibility is that the mutants are misexpressing a gene encoding a transcription factor that is activated in response to a hormone that controls tillering and height, similar to *tb1* and *gt1*.

Uneven patterning in the epidermal cell and stomata in the mutants could indicate a defect in cell differentiation. In order to further investigate cell differentiation pattern, the nuclei and cell wall can be stained using propidium iodide visualized with a confocal microscope. If the mutants are defective in cell wall differentiation, we would expect to see random cell wall formation. Visualization of the nuclei would further prove if the cells have divided in random formation when compared to the wild type controls.

Molecular data obtained from the *Mu*-library, together with the results obtained from SNPs, have proven that the candidate gene for *grass* and *mini-me* has yet to be identified. The allelism test will be verified once the crosses from the 2011 winter greenhouse are planted out.

The *mini-me* and *grass* mutants are extreme in their phenotype and the fact that they are the result of a single-gene mutations points to an unusual degree of pleiotropy. Results presented in this thesis provide evidence against the involvement of more downstream effectors in the hierarchy of possible signals.

In the future, the mutation line should be further back-crossed into a known homozygous inbred line such as W22 for at least four generations to reduce the copy number of *Mu* elements so that fewer *Mu* elements need to be considered for the co-segregation analysis. It will be a good plan to include at least two or three individual plants of the same mutant for the *Mu*-454 sequencing after back-crossed to avoid discrepancies such as incomplete sequencing of *Mu*-insertions in generating the *Mu*-library.

The mutation that caused *mini-me* and *grass* could be a spontaneous mutation. Therefore, a map-based followed by positional cloning approach or with SNPs with more mutant individuals instead of 25 mutants to obtain a higher resolution of mapping location. Although time and space consuming, would be more reliable than a providential event.

APPENDIX
FIGURES AND PRIMERS

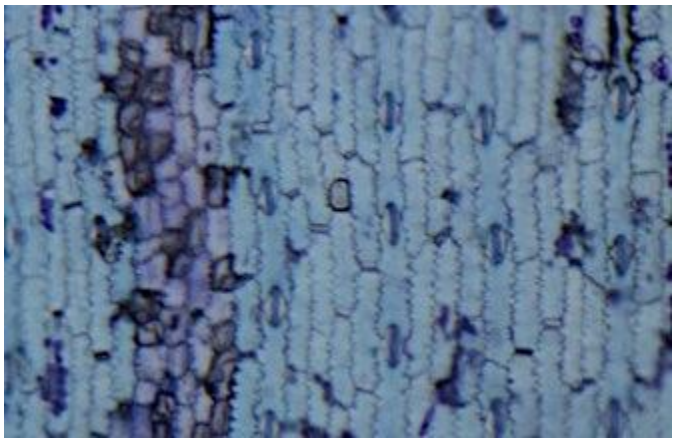

Figure A-1. Adaxial of wild-type,W22, showing purple stained bulliform cells

Table A-1. Nested *Mu* primers used to amplify adjacent DNA segments

Primer	Sequence (5' – 3')
TIR6	AGAGAAGCCAACGCCAWCGCCTCYATTTCGTC
TIR8.1	CGCCTCCATTTCGTCGAATCCCCTS
TIR8.2	CGCCTCCATTTCGTCGAATCCSCTT
TIR8.3	SGCCTCCATTTCGTCGAATCCCKT
TIR8.4	CGCCTCCATTTCGTCGAATCACCTC

Table A-2. Co-segregation primers for *Mini-me*

Name	Sequence
Zmmim-3.1-U144	CATTGCTCGTCTCTTTGGTCACGC
Zmmim-3.1-L1643	TCTCCACCGTCATCGCCATTGCT
Zmmim-3.2-U367	TAGGTTGCGAGAAAGCCAGTCCCT
Zmmim-3.2-L2390	ACTCCCAACGACAGCGAGAAGTGA
Zmmim-3.3-U289	TAACTCGGCTCGCTTGCTCATGTC
Zmmim-3.4-U328	AGAAGCCCGATTATGGACGCTGTGT
Zmmim-3.4-L1460	GTAGACCCAGTCACGATCCTAAAATCC
Zmmim-3.5-U309	TCACTGGGGTTCACTCCTCTTGC
Zmmim-3.5-L1307	CCATTTGGCTGCTCTGTATTTGTAATCC
Zmmim-3.6-U327	GGAGAGGGGGTAACAAAGTAAAGAGC
Zmmim-3.6-L1266	CACTTTTTCCTGCTACACCGTAGTGC
Zmmim-3.7U95	TCTTCGCACACGCACTCCACAC

Table A-2. Continued.

Name	Sequence
Zmmim-3.7-L1371	TATGTCCCCCCAGTTTCGTCGTCT
Zmmim-3.8-U148	TAAGGCGTGATGTGGGTGGGGAA
Zmmim-3.8-L937	CTGTGGGCTTCAACAATATACCATCCG
Zmmim-3.9U59	TCACCGCTTCGCTCAGTATCGCTT
Zmmim-3.9-L1340	TGTCGGATTGGTGGGTCGGAAC
Zmmim-3.10-U181	ATCACCACCAGCAGTACCACAGGA
Zmmim-3.10-L1253	TCTCGGGTACAATTTCGGGTCGG
Zmmim-3.11-U525	AGACCGCTCTTTGTGCCGACTATG
Zmmim-3.11-L1811	TCCACCGCAGATTTTTGGGGACGA
Zmmim-3.12-U97	CAGACCGATCATGTGTAGCATCAGC
Zmmim-3.12-L1428	CTCGTGCGAAAAGCCATCACAGCAT
Zmmim-3.13-U302	GATTCGGTGTGGTCTCTTTGTAGGG
Zmmim-3.13-L1199	GAGGGGGAAAAACTTCAGTGGCAG
Zmmim-3.14-U97	CAGACCGATCATGTGTAGCATCAGC
Zmmim-3.14-L1446	AGTGCGATATAGGAATCCCTCGTGC
Zmmim-4.2-U233	CTCTGCGTGAGTGCGTGTTTGGAT
Zmmim-4.2-L1253	ACTGGGGCACACCTGTATTCTCC
Zmmim-4.3U26	GAGAAGGGCAAATCTGTCTAGTGGAG
Zmmim-4.3-L1446	ACAACCCGCCGTCTGTAACACC
Zmmim-4.4-U182	AGACCGCTTCAGTTTACCCACTTTGC
Zmmim-4.4-L1022	GAGATGGGAGAGGATAGAGATGGAC
Zmmim-5.1-U445	AGTCCAGCCAAGAGTCATCGGTAC
Zmmim-5.1-L952	CAATGGGCTAGTAGGGGTAACTCG
Zmmim-5.3-U642	ATTGCGGACATGGCTCGGTCTTG
Zmmim-5.3-L1338	GTGGGCTCCGACAAGTGTGGTA
Zmmim-5.4-U275	CTAGCCAAACAGGATATTTGCTGAGTAC
Zmmim-5.4-L1151	TTTCCGACTATTACCGACCGTTTTCATTC
Zmmim-6.1-U517	CTCCGCCTTGAATCTCCATCAGATC
Zmmim-6.1-L1234	AGGGATCAGGAGCCACGGTGT
Zmmim-6.2-U574	TAAGGGGGAGTAAGCGGACAGCAA
Zmmim-6.2-L1120	TAGGCGTGAGGCGTATCGTCTTC
Zmmim-7.1-U343	GTGTGCCAATACTCCTCCTAGTCC
Zmmim-7.1-L1106	AAGAGCGACGGGATGATGCTGTAG
Zmmim-7.2-U242	ACAGCCGCCCTTCCAGATGGT
Zmmim-7.2-L1272	TCTAGCCGTGCCAAATGTCAAATATGG
Zmmim-7.3-U591	CACAGCCAACGAGTACACGAACTTG
Zmmim-7.3-L1447	AAGCCCCGAACACACTGACCACT
Zmmim-7.4-U464	ACTATGCTGTGTACTTGGTAGTTTGAAC
Zmmim-7.4-L1330	CTCAGCGTTACAAGTCAACTAGAACA
Zmmim-8.1-U530	AGGGGGAGGAGATGGAGTAGGAA
Zmmim-8.1-L1404	GAACTGGTGGGCTTAGTGGTTGG

Table A-2. Continued.

Name	Sequence
Zmmim-8.2-U140	TAACGGCGTGTTGGAATCTTGATGCG
Zmmim-8.2-L1355	CTATTTCCGACGAGTTATCCACGACG
Zmmim-8.3-U636	AAAACCCTCTCCTCTCTCATCCGC
Zmmim-8.3-L1436	TGGTGGGGTGGGATAGCACACT
Zmmim-8.4-U618	AATCCGCCATACCCGTGCCCTAAT
Zmmim-8.4-L1003	TAAAGCCGCCAAGTCTGAGGTGAG
Zmmim-8.5-U594	GTATGGCTCTTTGTACTGCTCCAGC
Zmmim-8.5-L1160	TCATCGTCGCCTCCAACCCTGT
Zmmim-8.6-U306	TGAAGGGAGATGTGAGCACCGACT
Zmmim-8.6-L1145	TTCTGCTGCTGTAGGTGTGGGTGT
Zmmim-8.7-U476	GGTTGGGCTGAGGTTATTTGGTCTG
Zmmim-8.7-L1263	AGACTCGCCAAACTGCTGCCC
Zmmim-9.1-U414	TAACGGTGGAGAAGGTCAAGTCGG
Zmmim-9.1-L767	TACCTCTCGCCCCCACTGCC
Zmmim-9.2-U606	CTGCCGCTGTCACAGAAACCCA
Zmmim-9.2-L930	TGGTGCCCTCGTCAAAGTGTAGC
Zmmim-9.3-L1090	CGTACGGCACCTTATTTCAATCTCGC
Zmmim-9.4U72	GGAGCCGTTCTCTTTCCCTTCATAT
Zmmim-9.4-L1273	CTTGGGTGGATGAGATGTCTGAAAAAC
Zmmim-9.5U62	TCACCCCCAAAATCTTCCACATGCG
Zmmim-9.5-L766	CCTTCCCCAGTCCCCACTACC
Zmmim-9.6-U632	TTTGCGGGACCTTTTTGCTGCTGC
Zmmim-9.6-L988	GGACCCGATACATGCTAACTAATGGAG
Zmmim-9.7-U523	TGTCGGGAAGAAGGGCTAGGGTTT
Zmmim-9.7-L1239	GTCTGCTCGGTTCGCTGTCTAACT
Zmmim-10.1-U80	AGAGGCTGGAATCACTCGTGGACT
Zmmim-10.1-L1264	TGCGGCGACCAGATTAGCAACC
Zmmim-10.2-U664	ATAGCCAACAGAACTACGACCAGTGG
Zmmim-10.2-L124	GATACCCGCCCACCTTCTTTAAGTTACT
Zmmim-10.3-U620	GTTGGCGTATGTAGCATACCGTACAG
Zmmim-10.3-L1095	GAGGGGAGAGAGAAAGATCAGAGC
Zmmim-10.4-U585	CGTCCCGTTTTCATCCCTACATCAAC
Zmmim-10.4-L1329	AAACCCCCCAAATCCAGTTACACCC
Zmmim-10.5-U207	TCAGCGGCATTACTGGCAGATTCCAT
Zmmim-10.5-L1078	CTTCGGGGTCGTTCACGCTCT
Zmmim-10.6-U506	TGACCCCACCTGTCAGTAAAGTTACC
Zmmim-10.6-L885	TCACGCCGACCACCACCGAAAATA
Zmmim-10.7-U681	GTTCGCCCAGGTCTACTCCTATCT
Zmmim-10.7-L1191	GAGGACCCATCACACTAACTTGTCAC
Zmmim-4.3r-U367	TCTTGGGACGGAGGTAGTATGTCC
Zmmim-4.3r-L1565	TCAGGGGAGACCATAACACGGGA

Table A-2. Continued

Name	Sequence
Zmmim-4.4r-U377	AGGTCGCACAACAGCAAAGGCTAG
Zmmim-4.4r-L1364	TTTCGCTCCATCGTGTTGTTCTTTCTG
Zmmim-4.11r-U93	ATAGGCACAGTATGGGACAGCGAC
Zmmim-4.11r-L1164	ACCGCCCCTTCCTCCGATTTGTT
Zmmim-4.12r-U354	AAGCCGAGTCCACCACCAAGCAT
Zmmim-4.12r-L820	TTTCGCCGTCTTATCCCTTCGTCC
Zmmim-5.1r-U104	AACCCGACCCATTGCCATCCCTAT
Zmmim-5.1r-L1532	TTCCCCTTCCTCCTCCTCGTCAT
Zmmim-5.2r-U738	CTTGCCATCCATGAACAACCCAGAG
Zmmim-5.2r-L1800	GTCGCCCAATTCGTTTACCTCCTC
Zmmim-6.1r-U260	ACTCGGTCAAGCAAGTAGTTCTGG
Zmmim-6.1r-L1773	CTTGGCATGGAGTCATAACATGGTC
Zmmim-7.1r-U507	GTTGCGTCCCTGTTTACATGATCTG
Zmmim-7.1r-L1099	GTTTGGCGACAACAAGGAGCAGTG
Zmmim-8.3r-U132	GTTGGGACCAGAGAGGAACAACTTTT
Zmmim-8.3r-L1245	AAAACGGCAATGGTTAGGGTATCCAC
Zmmim-8.6r-U576	GGTTGGGCTGAGGTTATTTGGTCTG
Zmmim-8.6r-L1525	GTTGCGGACAGTCTAAGAGTGGTCT
Zmmim-9.3r-L1373	CTTGGGTGGATGAGATGTCTGAAAAAC
Zmmim-10.1r-U374	ATCCGCAAGGAGGTCTTCGTCTC
Zmmim-10.1r-L1017	CGTCCCGTTTTCATCCCTACATCAAC

Table A-3. Co-segregation primers for *Grass*

Name	Sequence
Zmgra_2.2-U308	CTAACTCGGTGCTAAAGGTGTTGGTG
Zmgra_2.2-L995	GAGATGCGTGATGTTGCTTGCCAC
Zmgra_2.3-U481	AAACTGCTTTGCTCCATTTCTCTCGC
Zmgra_2.3-L1042	AGATCGTGGATGCCTCCTGGTG
Zmgra_2.4-U488	GTCAGCCTTACCTAACGCAAGCC
Zmgra_2.4-L681	CTCTCGCTCTCGTGGACTGACT
Zmgra_2.5-U394	TAGACCGTTTTCACCGTAAAAGGCACA
Zmgra_2.5-L1061	TTTGAGGGAACTTGATGACTGCTCG
Zmgra_2.6-U279	TGAAGGGAAACAAGTAGCAACCATGAAC
Zmgra_2.6-L627	GGACTCCAGCAGGCAGTCCAA
Zmgra_2.7-U130	GCAACGGAGGACATTTATACACACAT
Zmgra_2.7-L1016	CTTCACCCTGGTTCAGATTTCCTTAT
Zmgra_3.2-U192	GAGAGGGGAGATTCGGTGTGGT
Zmgra_3.2-L988	GAGTAGGGGAAGAGGTGCTGTC
Zmgra_6.4-U127	ATAGGTTCGGTTTGGTTCGGCTCG
Zmgra_6.4-L1057	GAACTCCGTGTTCGTCTCTGGGTA
Zmgra_6.6-U276	GATATTGAGGATTATGCCACCCTACCA

Table A-3. Continued.

Name	Sequence
Zmgra_6.6-L997	TCTCACTTTCGTATAGAGATAGGTCAGG
Zmgra_6.7-U113	GAGACCCCTCACACACTCACAGA
Zmgra_6.7-L1072	GATAGGCAGAGTGGAGTCTTGTAGTG
Zmgra_7.1-U113	GAGACCCCTCACACACTCACAGA
Zmgra_7.1-L903	GACACGACGAGCACACAGAGATTG
Zmgra_7.2-U228	GTCTAAGCGATCTTCACCATAATACAACG
Zmgra_7.2-L687	TGAGGAGGCGTTGAGGAACTTGAG
Zmgra_8.1-U412	AAATCCGCCATACCCGTGCCCTAA
Zmgra_8.1-L900	AAGAAGCAAGTACCTGGTTCAGAACTC
Zmgra_9.1-U335	GCTCGGCTCGTTTCCACTCCTA
Zmgra_9.1-L1082	CATTCTCGGCACATATCTCGTCACTG
Zmgra_10.2-U373	AAATCCCACTCGCCAACTCACCCT
Zmgra_10.2-L904	TACCTCCGAGACCGAGAAGCATTCTT
Zmgra_10.6-U46	AGATTGGTGCGTCCACACGAGAGT
Zmgra_10.6-L831	GTATCCGTCCCGTTTTCATCCCTAC
Zmgra-2.2r-U92	GTTTAGCAAGGTCAGGAGATGGTGG
Zmgra-2.2r-L1037	GATGGGACTGTTTGTTTGTGGGACG
Zmgra-2.5r-U682	TTGCCGCCTTGCCTCCACTCCA
Zmgra-2.5r-L807	GTGGGGACTGGAAACGTGGGGT
Zmgra-2.6r-U117	ACCACCTGATGCCATTTGAACTGGAG
Zmgra-2.6r-L1375	CTGCCGCTGCTTTGCTTTGCTC
Zmgra-2.7r-U331	CAACGGAGGACATTTATACACACATAGGT
Zmgra-2.7r-L819	ACGCCCGACATCAGCCTCGTAT
Zmgra-6.4r-U548	CCTACGGTCCTACCTGGCTACC
Zmgra-6.4r-L1006	GGAGCGGAGGTTGAGGGACTTGA
Zmgra-6.6r-U620	GAATCCGCTTACTAAAAGGCTTCCATCC
Zmgra-6.6r-L1123	CTAGCGATGTTGGTGGCTTTCCTC
Zmgra-6.7r-U314	AGACCCCTCACACACTCACAGACA
Zmgra-6.7r-L1098	GACGAGCACACAGAGATTGGTTGG
Zmgra-7.1r-U295	GATGGGGGATTGGGATTTGGGACT
Zmgra-7.1r-L786	TAGTGCCCTAGTTCCTGTCCAAGC
Zmgra-7.2r-U526	TAAGGGGCAGGTGGAACTCTCC
Zmgra-7.2r-L827	GAGGAGGCGTTGAGGAACTTGAG
Zmgra-9.1r-U436	CTCGGCTCGTTTCCACTCCTAGGT
Zmgra-9.1r-L973	CTCGGGCATCGGCAGTGGGAA
Zmgra-2.1-chr6B73-U551	CTACCGCTCTCCATGAGTGGCAAAT
Zmgra-2.1-chr6B73-L1121	GAAGGGGGAAGAAGAAAAGGCTGC
Zmgra-2.2r2-U510	AACTCGGTGCTAAAGGTGTTGGTGTT
Zmgra-2.2r2-L1465	ACTCGCAGGTCTGGGAGATTCATTC
Zmgra-2.5r2-U297	TATGGCAAAAATGTACGACCAGATCAAA
Zmgra-2.5r2-L1639	CACACGGTTCTACTATGTCCAACA

Table A-3. Continued.

Name	Sequence
Zmgra-2.6r2-U408	CATGCCGCAATGTAGAATGCTTCAATC
Zmgra-2.6r2-L1595	GAAGGCGACAATCTGTTGCTCGG
Zmgra-2.7r2-U211	ATTCGGAAGAGAAGCGTTGACTCG
Zmgra-2.7r2-L1353	ATCTTGCCGTGTAGACACTTCGCA
Zmgra-6.4r2-U650	TACGGTCCTACCTGGCTACCTTC
Zmgra-6.4r2-L1542	CTCCCCAAACATAGTCAGCGGAAG
Zmgra-6.6r2-U162	TAAGCCCTCTTCTGAATCATTACCTCCC
Zmgra-6.6r2-L1696	ATCGGGTTTATGTTCGTGCTCTCGGA
Zmgra-6.7r2-U27	TGACCGTGGTTAGTAGAGTCTCAATCTG
Zmgra-6.7r2-L1425	TCGGCGAGCTGTGGTAAAGCGTA
Zmgra-7.1r2-U396	ATGGGGGATTGGGATTTGGGACTTG
Zmgra-7.1r2-L1713	CTGTGGCGGAACTGCGTGAATTATTC
Zmgra-7.2r2-U158	CTAGGGCTCTCTTACAGAGGGTTG
Zmgra-7.2r2-L1682	CAGTGCCCACATCATGCCAAACTAC
Zmgra-9.1r2-U2	TCATCGGTGGAAGAGGAGACAGACT
Zmgra-9.1r2-1802	TGAGCCGTTCAAAGCGTGCCAAAAC

LIST OF REFERENCES

Arite T, Iwata H, Ohshima K, Maekawa M, Nakajima M, Kojima M, Sakakibara H, Kyozuka J (2007). DWARF10, an RMS1/MAX4/DAD1 ortholog, controls lateral bud outgrowth in rice. Plant J 51: 1019–1029.

Ashikari M, Sasaki A, Ueguchi-Tanaka M, Itoh H, Nishimura A, Datta S, Ishiyama K, Saito T, Kobayashi M, Khush GS, Kitano H, Matsuoka M (2002). Loss-of-function of a rice gibberellins biosynthetic gene, GA20 oxidase (GA20ox-2), led to the rice green revolution. Breed Sci 52: 143–150.

Ashikari M, Sakakibara H, Lin S, Yamamoto T, Takashi T, Nishimura A, Angeles A, Qian Q, Kitano H, Matsuoka M. (2005). Cytokinin oxidase regulates rice grain production. Science 309: 741-745.

Benfey PN, Linstead PJ, Roberts K, Schiefelbein JW, Hauser M-T, Aeschbache, RA (1993). Root development in *Arabidopsis*: four mutants with dramatically altered root morphogenesis. Development 119: 57-70.

Benito MI, Walbot V (1997). Characterization of the maize *Mutator* transposable element MURA transposase as a DNA-binding protein. Mol Cell Biol 17: 5165–5175.

Bennetzen JL (1984). Transposable element *Mu1* is found in multiple copies only in Robertson's *Mutator* maize lines. J Mol Appl Genet 2: 519–524

Beveridge CA, Symons GM, Murfet IC, Ross JJ, Rameau C (1997). The *rms1* mutant of pea has elevated indole-3-acetic acid levels and reduced root-sap zeatin riboside content but increased branching controlled by graft-transmissible signal(s). Plant Physiol 115: 1251–1258.

Bishop GJ, Nomura T, Yokota T, Harrison K, Noguchi T (1999). The tomato DWARF enzyme catalyses C-6 oxidation in brassinosteroid biosynthesis. Proc Natl Acad Sci USA 96:1761–1766.

Bleckman A, Simon R (2009). Interdomain signaling in stem cell maintenance of plant shoot meristems. Mol Cells 27: 615–620.

Booker J, Sieberer T, Wright W, Williamson L, Willett B, Sternberg P, Turnbull C, Srinivasen M, Goddard P, Leyser O (2005). MAX1 encodes a cytochrome P450 family member that acts downstream of MAX3 /4 to produce a carotenoid derived branch inhibiting hormone. Dev Cell 8:443-449.

Bouwmeester HJ, Roux C, Lopez R, Guillaume B (2007).Rhizosphere communication of plants, parasitic plants and AM fungi. Trends Plant Sci 12: 224-230.

Chandler V, Rivin C, Walbot V (1986). STable. non-mutator stocks of maize have sequences homologous to the Mu1 transposable element. Genetics 114: 1007–1021.

Chandler VL, Walbot V (1986). DNA modification of a maize transposable element correlates with loss of activity. Proc Natl Acad Sci USA 83: 1767–1771.

Cheng YF, Dai XH, Zhao YD (2006). Auxin biosynthesis by the YUCCA flavin monooxygenases controls the formation of floral organs and vascular tissues in Arabidopsis. Genes Dev 20: 1790–1799.

Chuck GE, Cigan MA, Saeteurn K, Hake S (2007). The heterochronic maize mutant Corngrass1 results from over expression of a tandem microRNA. Nat Genet 39: 544-549.

Clark SE, Williams RW, Meyerowitz EM. (1997). The CLAVATA1 gene encodes a putative receptor kinase that controls shoot and floral meristem size in Arabidopsis. Cell 89, 575-585.

Cubas P, Lauter N, Doebley J, Coen, E. (1999). The TCP domain: a motif found in proteins regulating plant growth and development. Plant J 18: 215–222.

Doebley J, Stec A, Hubbard L (1997). The evolution of apical dominance in maize. Nature 386: 485–488.

Doebley J (1983). The taxonomy and evolution of Tripsacum and teosinte, the closest relatives of maize. Pp. 15-28 in Gordon DT, Knoke JK, Nault LR, eds., Proc Intl Maize Virus Disease Colloquium and Workshop. The Ohio State University, Ohio Agricultural Research and Development Center, Wooster, Ohio.

Doust A (2007a). Architectural evolution and its implications for domestication in grasses. Ann Bot 100: 941–950.

Doust A (2007b). Grass architecture: genetic and environmental control of branching. Curr Opin Plant Biol 10: 21–25.

Dun EA, Ferguson BJ, Beveridge CA (2006). Apical dominance and shoot branching: divergent opinions or divergent mechanisms? Plant Physiol 142: 812–819.

Eveland AL, McCarty DR, Koch KE (2008). Transcript profiling by 3'-untranslated region sequencing resolves expression of gene families. Plant Physiol 146:32-44.

Ferguson BJ, Beveridge CA (2009). Roles for auxin, cytokinin, and strigolactone in regulating shoot branching. Plant Physiol 149: 1929-1944.

Finlayson FA (2007). Arabidopsis TEOSINTE BRANCHED1-LIKE 1 regulates axillary bud outgrowth and is homologous to monocot TEOSINTE BRANCHED1. Plant Cell Physiol 48: 667–677.

Gale MD, Law CN, Marshall GA, Worland AJ. (1975). The genetic control of gibberellic acid insensitivity and coleoptile length in “dwarf” wheat. Heredity 34:393–399.

Galinat WC (1954). Corn grass: I. corn grass as a prototype or a false progenitor of maize. The American Naturalist 8: 101-104.

Gallavotti A, Yang Y, Schmidt RJ, Jackson D (2008). The relationship between auxin transport and maize branching. Plant Physiol 147:1913–1923.

Gomez-Roldan V, Fermas S, Brewer PB, Puech-Page`s V, Dun EA, Pillot JP, Letisse F, Matusova R, Danoun S, Portais JC (2008). Strigolactone inhibition of shoot branching. Nature 455: 189–194.

Gray JE, Stuart C, Lee H (2008). Intercellular peptide signals regulate plant meristematic cell fate decisions. Sci Signal 49:e53.

Gray WM., Kepinski S., Rouse D., Leyser O, Estelle, M (2001). Auxin regulates SCF (TIR1)-dependent degradation of AUX/IAA proteins. Nature 414:271-6.

Grove MD, Spencer GF, Rohwedder WK, Mandava N, Worley JF (1979). Brassinolide, a plant growth-promoting steroid isolated from Brassica napus pollen. Nature 281:216–17.

Harberd NP, Freeling M (1989). Genetics of dominant gibberellin-insensitive dwarfism in maize. Genetics 121:827–38.

Hulbert SH, Richter TE, Axtell JD, Bennetzen JL (1990). Genetic mapping and characterization of sorghum and related crops by means of maize DNA probes. Proc Natl Acad Sci USA 87: 4251-4255.

Ikeda A, Tanaka MA, Sonoda Y, Kitano H, Koshioka M, Futsuhara M, Matsuoka M, Yamaguchi J.2001. Rice, a constitutive gibberellin response mutant, is caused by a null mutation of the SLR1 gene, an ortholog of the height-regulating gene GAI/RGA/RHT/D8. Plant Cell 13: 999-1010.

Jackson D, Hake S (1999). Control of phyllotaxy in maize by the abphyl1 gene. Development 126: 315-323.

James MG, Scanlon MJ, Qin M, Robertson DS, and Myers AM (1993). DNA sequence and transcript analysis of transposon MuA2, a regulator of mutator transposable element activity in maize. Plant Mol Biol 21: 1181–1185.

Jasinski S, Piazza P, Craft J, Hay A, Woolley L, et al (2005). KNOX action in Arabidopsis is mediated by coordinate regulation of cytokinin and gibberellin activities. Curr Biol 15:1560–65.

Jin J, Huang W, Gao J-P, Yang J, Shi M, Zhu MZ, Luo D, Lin HX (2008). Genetic control of rice plant architecture under domestication. Nat Genet 40: 365-369.

Jones PM, George AM (2004). The ABC transporter structure and mechanism: perspectives on recent research. Cell Mol Life Sci 61:682–99.

Kebrom TH, Brutnell TP (2007). The molecular analysis of the shade avoidance syndrome in the grasses has begun. J Exp Bot 58: 3079–3089.

Kellogg EA (1998). Relationships of cereal crops and other grasses. Proc Natl Acad Sci USA 95: 2005-2010

Kerstetter KE, Vollbrecht YE, Lowe B, Veit B, Yamaguchi J, Hake S (1994). Sequence analysis and expression patterns divide the maize knottedl-like homeobox genes into two classes. Plant Cell 6: 1877-1887.

Khamlichi RC, Huntley R, Jacqmard A, Murray JH (1999). Cytokinin activation of Arabidopsis cell division through a D-type cyclin. Science 283: 1541-1544.

Khush GS (2001). Green Revolution: The way forward. Nature Rev Genet 2: 815–822.

Koka CV, Cerny RE, Gardner RG, Noguchi T, Fujioka S, Takatsuto S, Yoshida S, Clouse SD (2000). A putative role for the tomato genes DUMPY and CURL-3 in brassinosteroid biosynthesis and response. Plant Physiol 122:85–98.

Le QH, Wright S, Yu Z, Bureau T (2000). Transposon diversity in Arabidopsis thaliana. Proc Natl Acad Sci USA 97: 7376–7381.

Leyser O (2003).Regulation of shoot branching by auxin. Trends Plant Sci 8: 541–545.

Lincoln C, Britton JH, Estelle M (1990). Growth and development of the axr1 mutants of Arabidopsis. Plant Cell 2: 1071–1080.

Lisch D (2002). Mutator transposons. Trends Plant Sci 7: 498–504.

Mandava B.N. (1988). Plant growth promoting brassinosteroids.Annu. Rev. Plant Physiol. Plant Mol. Biol 39:23–5

May EW, Craig NL (1996). Switching from cut-and-paste to replicative Tn7 transposition. Science 272: 401–404.

Mayer KFX, Schoof H, Haecker A, Lenhard M, Jürgens G, Laux T (1998). Role of WUSCHEL in regulating stem cell fate in the Arabidopsis shoot meristem. Cell 95: 805-815.

McCarty DR, Carson CB, Stinard PS, Robertson DS (1989). Molecular analysis of viviparous-1: an abscisic acid-insensitive mutant of maize. Plant Cell 1: 523–532.

McCarty DR, Settles AM, Suzuki M, Tan BC, Latshaw S, Porch T, Robin K, Baier J, Avigne W, Lai Messing J, Koch KE, Hannah K. (2005).Steady-state transposon mutagenesis in inbred maize. Plant J 44: 52–61.

McClintock B (1950).The origin and behavior of muTable. loci in maize. Proc Natl Acad Sci USA 36: 344- 355.

McClintock B (1947). Cytogenetic studies of maize and Neurospora. Carnegie Inst Wash Year 46:146–152.

McLaughlin M, Walbot V (1987). Cloning of a muTable. bz2 allele of maize by transposon tagging and differential hybridization. Genetics 117: 771-776.

Monna L, Kitazawa N, Yoshino R, Suzuki J, Masuda H, Maehara Y, Tanji M, Sato M, Nasu S, Minobe Y (2002). Positional cloning of rice semidwarfing gene. sd-1: rice 'green revolution gene' encodes a mutant enzyme involved in gibberellin synthesis. DNA Res 9: 11–17.

Muller R, Bleckmann A, and Simon R (2008). The receptor kinase CORYNE of Arabidopsis transmits the stem cell-limiting signal CLAVATA3 independently of CLAVATA1. Plant Cell 20: 934–946.

Multani SM, Briggs SP, Mark SA. Chamberlin, Blakeslee JJ, Murphy AS, Johal JS. (2003). Loss of an MDR transporter in compact stalks of maize br2 and sorghum dw3 mutants. Science 302: 81-84.

Nomura T, Kitasaka Y, Takatsuto S, Reid JB, Fukami M (1999). Brassinosteroid/sterol synthesis and plant growth as affected by lka and lkb mutations of pea. Plant Physiol 119:1517–526.

Nomura T, Nakayama M, Reid JB, Takeuchi Y, Yokota T (1997). Blockage of brassinosteroid biosynthesis and sensitivity causes dwarfism in garden pea. Plant Physiol 113:31–37.

Ohyama K, Shinohara H, Ogawa-Ohnishi M, Matsubayashi Y (2009). A glycopeptide regulating stem cell fate in Arabidopsis thaliana. Nature 5: 578–580.

Paterson AH, Bowers JE, Bruggmann R, Dubchak I, Grimwood J, Gundlach H, Haberer G, Hellsten U, Mitros T, Poliakov A *et al.* (2009). The Sorghum bicolor genome and the diversification of grasses. Nature 457: 551-556.

Peng JR, Richards DE, Hartley NM, Murphy GP, Devos KM, Flintham JE, Beals J, Fish LJ, Worland AJ, Pelica F, Sudhakar D, Christau P, Snape J, Gale MD, Herberd NP (1999). Green revolution genes encode mutant gibberellin response modulators. Nature 400: 256–261.

Peng J, Carol P, Richards DE, King KE, Cowling RJ (1997). The Arabidopsis GAI gene defines a signaling pathway that negatively regulates gibberellin responses. Genes Dev 11: 3194–3205.

Pysh LD, Wysocka-Diller JW, Camilleri C, Bouchez D, Benfey PN (1999). The GRAS gene family in Arabidopsis: sequence characterization and basic expression analysis of the SCARECROW-LIKE genes. Plant J 18: 111–119.

Qin MM, Robertson DS, Ellingboe AH (1991). Cloning of the mutator transposable element MuA2, a putative regulator of somatic mutability of the a1-mum2 allele in maize. Genetics 129: 845–854.

Reilly CO, Shepherd NS, Pereira A, Schwarz-Sommer Z, Bertram I, Robertson D, Peterson PA, Saedler HS. (1985). Molecular cloning of the a1 locus of Zea mays using the transposable elements En and Mu1. EMBO J 4: 887-882.

Rhoades MW, Reinhart BJ, Lim LP, Burge CB, Bartel B, Bartel DP (2002). Prediction of plant microRNA targets. Cell 110: 513-520.

Riou-Khamlichi C, Huntley R, Jacqmard A, Murray JA (1999). Cytokinin activation of Arabidopsis cell division through a D-type cyclin. Science 283:1541–44.

Robertson DS (1978). Characterization of a mutator system in maize. Mutat Res 51: 21–28.

Rojo E, Sharma VK, Kovaleva V, Raikhel NV, Fletcher J (2002). CLV3 is localized to the extracellular space, where it activates the Arabidopsis clavata stem cell signaling pathway. Plant Cell 14: 969–977.

Sakakibara H (2006). Cytokinins: activity, biosynthesis, and translocation. Annu Rev Plant Biol 57:431–49.

Sasaki A, Ashikara M, Ueguchi-Tanaka M, Itoh H, Nishimura A, Swapan D, Ishiyama K, Saito T, Kobayashi M, Khush GH, Kitano H, Matsuoka M (2002). Green revolution: a mutant gibberellin synthesis gene in rice – new insight into the rice variant that helped to avert famine over thirty years ago. Nature 416: 701–702.

Schnable PS Ware D Fulton RS Stein JC Wei FS Pasternak S Liang CZ Zhang JW Fulton L Graves TA *et al.* (2009). The B73 Maize Genome: Complexity, Diversity, and Dynamics. Science 326: 1112-1115.

Settles AM, Holding DR, Tan BC, Latshaw SP, Liu, Suzuki M, Li L, O'Brien BA, Fajardo DS, Wroclawska EA, Tseung CW, Lai JS, Hunter CT III, Avigne WT, Baier JP, Messing JP Hannah CS, Koch KE, Becraft BE, Larkins BE McCarty DR. (2007). Sequence-indexed mutations in maize using the UniformMu transposon-tagging population. BMC Genomics 8:116.

Silverstone AL, Ciampaglio CN, Sun T-P (1998). The Arabidopsis RGA gene encodes a transcriptional regulator repressing the gibberellin signal transduction pathway. Plant Cell 10: 155-169.

Singleton WR (1951). Inheritance of Corn grass, a macromutation in maize, and its possible significance as an ancestral type. Am Nat 305: 81–96.

Siobhan A, Braybrook, Kuhlemeier C (2010). How a Plant Builds Leaves. Plant Cell 22: 1006–1018.

Takeda T, Suwa Y, Suzuki M, Kitano H, Tanaka MU, Ashikari MU, Matsuoka M, Ueguchi C (2003). The OsTB1 gene negatively regulates lateral branching in rice. Plant J 33: 513–520.

Teale WD, Paponov IA, Klaus Palme (2006). Auxin in action: signalling, transport and the control of plant growth and development. Nature Rev Mol Cell Biol 7: 857-859.

Trotochaud AE, Hao T, Wu G, Yang Z, Clark SE (1999). The CLAVATA1 receptor-like kinase requires CLAVATA3 for its assembly into a signaling complex that includes KAPP and a Rho-related protein. Plant Cell 11: 393-406.

Umehara M, Hanada A, Yoshida S, Akiyama K, Arite T, Takeda-Kamiya N, Magome H, Kamiya Y, Shirasu K, Yoneyama K (2008). Inhibition of shoot branching by new terpenoid plant hormones. Nature 455: 195–200.

Umehara M, Hanada A, Yoshida S, Akiyama K, Arite T, Kamiya KT, Magome H, Kamiya Y, Shirasu K, Yoneyama K, Kyozuka J, Yamaguchi S (2008). Inhibition of shoot branching by new terpenoid plant hormones. Nature 455: 195-200.

Vermerris W, Vreugdenhill D, Visser RGF (2001). mRNA localization in invitro grown microtubers of potato as a tool to study starch metabolism. Plant Physiol Biochem 39: 161-166.

Walbot V (2000). Saturation mutagenesis using maize transposons. Curr Opin Plant Biol 3:103–107.

Wang J, Roe B, Macmil S, Yu Q, Murray JE, Tang H, Chen C, Najar F, Wiley G, Bowers J, Sluys MAV, Rokhsar DS, Hudson ME, Moose SP, Paterson AP, Ming R. (2010). Microcollinearity between autopolyploid sugarcane and diploid sorghum genomes. BMC Genomics 11: 261.

Wang X, Chory J (2006). Brassinosteroids regulate dissociation of BKI1, a negative regulator of BRI1 signaling, from the plasma membrane. Science 313:1118–22.

Wang ZY, He JX. (2004). Brassinosteroid signal transduction–choices of signals and receptors. Trends Plant Sci 9:91–96.

Weil CF, Kunze R (2000). Transposition of maize Ac/Ds transposable elements in the yeast Saccharomyces cerevisiae. Nat Genet 26: 187–190.

Werner T, Motyka V, Laucou V, Smets R, Van Onckelen H, Schmulling T (2003). Cytokinin-deficient transgenic Arabidopsis plants show multiple developmental alterations indicating opposite functions of cytokinins in the regulation of shoot and root meristem activity. Plant Cell 15: 2532–2550.

Willige BC, Ghosh S, Nil C, Zourelidou M,. Dohmann EMN, Maier A, Schwechheimer C (2007). The DELLA domain of GA INSENSITIVE mediates the interaction with the GA INSENSITIVE DWARF1A gibberellins receptor of Arabidopsis. Plant Cell 19: 1209-1220.

Winkler RG, Freeling M (1994). Analysis of the autonomy of maize dwarf 1 action in genetic mosaics. J Hered 85: 377–80.

Woodhouse MR, Freeling M, Lisch D (2006). Initiation, establishment, and maintenance of heriTable. MuDR transposon silencing in maize are mediated by distinct factors. PLoS Biol 4: e339.

Woodhouse MR, Freeling M, Lisch D (2006). The mop1 (mediator of paramutation1) mutant progressively reactivates one of the two genes encoded by the MuDR transposon in maize. Genetics 172: 579–592.

Xu M, Zhu L, Shou HX, Wu P (2005). A PIN1 family gene, OsPIN1, involved in auxin-dependent adventitious root emergence and tillering in rice. Plant Cell Physiol 46: 1674–1681.

Yabuta T, Sumiki Y (1938). On the crystal of gibberellin, a substance to promote plant growth. J Agric Chem Soc Japan. 14:1526.

Yamamoto Y, Kamiya N, Morinaka Y, Matsuoka M, Sazuka T (2007). Auxin biosynthesis by the YUCCA genes in rice. Plant Physiol 143: 1362–1371.

Yamamuro C, Ihara Y, Wu X, Noguchi T, Fujioka S, et al (2000). Loss of function of a rice brassinosteroid insensitive1 homolog prevents internode elongation and bending of the lamina joint. Plant Cell 12:1591–606.

Yamamuro C, Ihara Y, Wu X, Noguchi T, Fujioka S, Takatsuto S, Ashikari M, Kitano H, Matsuoka Ml (2000). Loss of function of a rice brassinosteroid insensitive1 homolog prevents internode elongation and bending of the lamina joint. Plant Cell 12:1591–1605.

Yanai O, Shani E, Dolezal K, Tarkowski P, Sablowski R, Sandberg G, Samach A, Naomi O (2005). Arabidopsis KNOXI proteins activate cytokinin biosynthesis. Curr Biol 15:1566–71.

Yu J, Hu SN, Wang J, Wong GKS, Li SG, Liu B, Deng YJ, Dai L, Zhou Y, Zhang XQ et al (2002). A draft sequence of the rice genome (Oryza sativa L. ssp indica). Science 296: 79-92.

Zou JH, Zhang SY, Zhang WP, Li G, Chen ZX, Zhai WX, Zhao XF, Pan XB, Xie Q, Zhu LH (2006). The rice HIGH-TILLERING DWARF1 encoding an ortholog of Arabidopsis MAX3 is required for negative regulation of the outgrowth of axillary buds. Plant J 48: 687–696.

BIOGRAPHICAL SKETCH

Sharon Tan attended Tunku Abdul Rahman College, Penang, Malaysia and earned a diploma in electrical and electronic engineering in 2003. After graduation she attended Damansara Utama College, Penang, Malaysia into the American University Transfer Program (AUTP) and continued on to Linfield College, McMinnville, Oregon in 2005. In spring of 2007 she earned her B.Sc. in biology. Upon graduation she joined the marker assisted breeding lab at Nunhems Inc., Salem, Oregon in 2007. In 2008, she decided to go back to school to pursue a Master of Science and joined Dr. Wilfred Vermerris's lab at the University of Florida.